Review Article

Miscellaneous Azo Dyes: A Review on Recent Advancements and Applications

Waleed K. Mahdi[1], Enass J. Waheed [1], Hanan Adnan Shaker Al- Naymi[1], Shatha M. H. Obaid[1], Amer J. Jarade [1]and. Marwan Mahmood Saleh[2]

[1] Department of Chemistry -College of Education for Pure Science / Ibn Al-Haitham, University of Baghdad, Iraq.

[2] Department of Medical Physics, College of Applied Sciences, University of Anbar, Iraq.

Corresponding email: ah.marwan_bio@uoanbar.edu.iq waleed.k.m@ihcoedu.uobaghdad.edu.iq , enass.j.w@ihcoedu.uobaghdad.edu.iq , hanan.a.s@ihcoedu.uobaghdad.edu.iq

, shatha.m.h@ihcoedu.uobaghdad.edu.iq

, amir.j.j@ihcoedu.uobaghdad.edu.iq,

Abstract:

The dyes Azo have a lengthy history and are a vital part of our daily lives. There are numerous potentials uses for these substances and their derivatives in various industries and environmental and biological research. In this study conversion of various azo compounds into other derivatives, complexes, and polymers was accomplished. This review included examining the chemistry reactions, synthesis, and applications of azo dye ligands and their complexes, mentioned spectral, analytical, thermal, and morphology methods of investigation, and confirmed by mass fragment mechanisms for some azo dyes and metal complexes. One of the aims of this review is to explain the role of these azo dye derivatives and the effect of metal complexes on leather which exhibits high light fastness, wash fastness, and rubbing fastness. The interaction of DNA has also been achieved. New metal complexes (Co (II), Ni (II), Cu (II), and Zn (II) azo ligands derived from 4-amino antipyrine and 4-aminoacetophenone are reported. The nature of the compounds has been studied followed by methods of continuous contrast, Beer's law, and molar ratio. Analytical methods and spectra revealed the octahedral geometry of the complexes. The azo dye ligand and its metal (II) complexes possess appreciable microbial activities. Novel heterocyclic compounds and its complexes have been investigated. The relationship between the HOMO-LUMO gap and antibacterial activity was investigated computationally. Improved understanding of binding mechanisms was shown by the comparative molecular docking investigations. This review demonstrated the utilization of the polycrystalline Zn (II) metal complex as a sensitizer in organic dye-sensitized solar cells. Quinolinyl-azo-naphthol (HL) is a selective turn-on chemosensor for Al^{3+} in the presence of other ions, exhibiting a 750-fold rise in emission at 612 nm following activation at visible light (537 nm). The reported limit of detection (LOD) for the 3σ technique is 0.69 nM.

During this review it was proven that the effective production of palladium nanoparticles with guar gum as a stabilizer and their use as a catalyst in reduction processes and azo dye degradation. The investigation describing and assessing thiazolyl azo ligand complexes with specific metal ions has been presented.(Zn (II), Cu (II), Co (II), and Ni (II)) complexes with azo ligands generated from metoclopramide hydrochloride were examined for their industrial and biological applications in cotton fabric dyeing, as well as for light and cleaner firmness. Additionally, the evaluation of the ligand and their complexes' antimicrobial and antifungal capabilities revealed that the ZnL molecule had the strongest antibacterial activity. The application characteristics of thiophene-derived dispersion dyes complexed with Zn, Cu, and Co metal on (polyester and Nylon 6.6), showed good to excellent light fastness, good to excellent wash fastness, excellent fastness to perspiration and sublimation, and good levelness on both materials with varying shades of brown and violet. The azo benzoic acid ligand derived from 2,4-dimethylphenol and 4-aminobenzoic acid has been identified by several spectroscopic methods and has been used as dispersion dyes on cotton textiles to test the antibacterial properties of the chemicals generated against a range of bacteria and fungus. Each primed complex has been proposed to have a tetrahedral geometrical structure for the obtained datum. There have been reports on the use of azo dyes in combination with nickel and its uses in dye-sensitized solar cells. Ten complexes of metals including Zn (II), Cu (II), Cd (II), Ni (II), and Co (II) as well as Phloroglucinol and antipyrine were used to create two unique azo-colorants, which were isolated and examined using a variety of techniques, wool, polyamide, and poly acetate fibers exhibit coloristic activity toward H_3L^1 and H_3L^2 as well as their metal complexes, demonstrating their strong resistance to UV radiation. Both in static and dynamic settings, the H_3L^2 compound exhibited a good sorption activity towards heavy metal cations from aqueous solutions of trace concentrations. A particular combination of selected transition metal ions is complexed with the azo compound, which is obtained from the (2-hydroxy quinoline: synthesis, characterization, thermal analysis, and antioxidant activity). These compounds' reactive oxygen entity degradation was evaluated with the DPPH radical and subsequently compared to gallic acid, a standard naturally occurring antioxidant. Finally, this review explains the metal chelates of the azo dye derivative sulfafurazole through synthesis, structure confirmation, molecular docking simulation, antibacterial, anticancer, and application in bioinorganic chemistry.

Keywords: Azo dyes, Synthesis, Antimicrobial, Applications, Complexes.

Introduction:

The pre-aniline era, which began at the beginning and lasted until 1856, can be considered the first of two major periods in the history of dyeing. The second epoch is the post-aniline. The former's distinctive appearance was partly because some of the colors were based on plants and animals that produce dyes. Madder root was used to make most of the vegetable dyes used in Asia and Europe. The blue dye still used in jeans today is created in India using the leaves of the indigo plant and a vivid red dye **[1-4].** Azo dyes are substances with two mono- or polycyclic aromatic systems connected to one or more azo groups (-N=N-). Because azo dyes have color, unlike most organic compounds, azo compounds have various uses. In the leather and textile industries, they play a significant and widespread role as coloring agents, and many applications1 as shown in **Figure -1 [5].**

Fig 1: Azo dyes applications

According to the precise structure of the molecule, azo dyes can theoretically produce a full rainbow of hues. Azo dye compounds can actually be found in the colors yellow, orange, red, brown, and blue. Different substitutions for aromatic rings lead to variations in the system's degree of conjugation in the azo dye, which affects color Known to be. Numerous azo dyes have been used in complexometric titrations and as chromogenic reagents for colorimetric measurements. Azo metal complexes were applied to the skin, and tests were performed on their ability to maintain color. **[5,6**]. The majority of azo dyes are made from diazonium salts, and they make up 60–70% of all industrial dyes used today. The produced azo dyes with chromium complexes are colored and have found extensive use in a variety of practical contexts, including optical storage technology, photo-electronic applications, printing systems, fiber coloring, photo-electronic applications, and biological reactions**.[7]** The review paper tries to concentrate on how azo dyes and their complexes have been categorized and synthesized using of some different techniques over the last ten years. Due to their expanding commercial and biological potential, azo dyes are frequently used as the primary scaffold in organic compounds, and Auxiliary methods used to study the nature of azo dyes include (XRD: X-ray diffraction), Scanning Electron Microscope (SEM) images, Transmission Electron Microscopy (TEM) images,(XPS: X-Ray Photoelectron Spectroscopy), Energy Dispersive X-Ray (EDX), (UV-vis DRS: UV-vis Diffuse Reflectance Spectroscopy), Photoluminescence intensity, Adsorption / Desorption (AS Ap analyzer), Ion Chromatograph, melting points, Electron Spin Resonance (ESR), FT-IR- ATR spectra,^{13}C-NMR ,^{1}H-NMR, elemental microanalysis(C.H.N.S.O), LC-Mass) analysis for ligand. Elemental analysis, atomic absorption of flame, as well as conductivity, magnetic quantifications for complexes, molar ratio, transient Photocurrent response plot, (EIS: Electrochemical Impedance Spectroscopy), (TGA-DTA and DSC: thermal gravimetric analysis - differential thermal analysis, and Differential scanning calorimetry), SEM and TEM (scanning electron microscopy and tunneling electron microscopy). The current review focuses on discussing Azo dye's ligands and complexes synthesis as well as various applications in some different industries and their applications in biomedicine.

Azo dyes compounds and metal ions complexes synthesis and applications studies:

In (2017, Nasir. A et al) **[8]** have been synthesized new Chromium (III) complexes with new acid dye ligands from 4-Amino-1-(psulphophenyl)- 3-methyl-5-pyrazolone diazonium salt as well phenolic couplers as shown in (**Scheme – 1**).

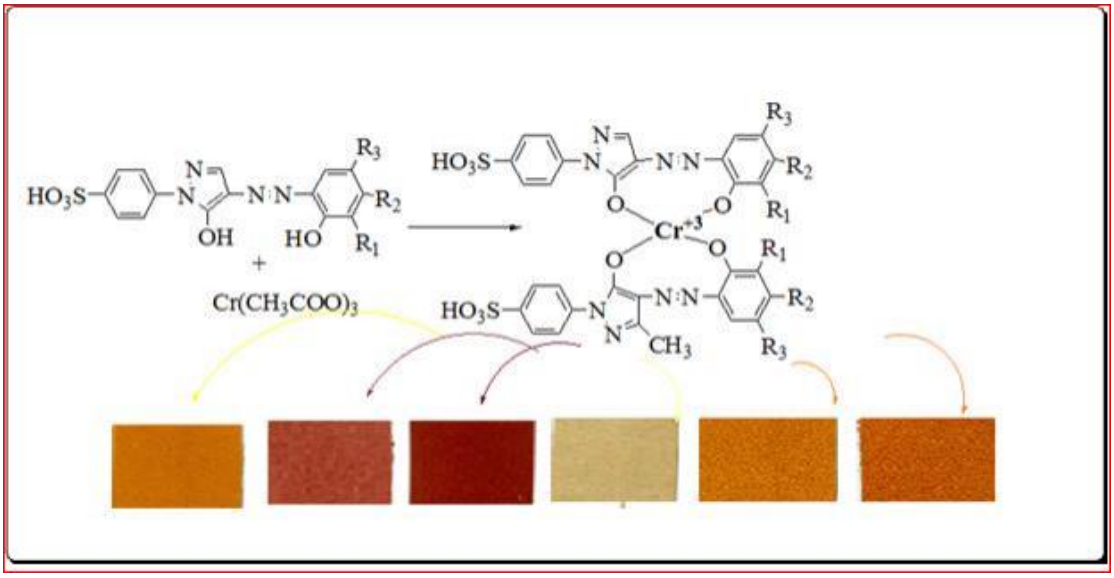

Scheme -1: Preparation of new Chromium (III) complexes with 4-Amino-1-(psulphophenyl)-3-methyl-5-pyrazolone diazonium salt coupled with different phenolic couplers.

All these compounds are described by chemical and physical methods, like 1H-NMR, Ft-IR, and UV-visible spectrophotometric studies. The octahedral geometry has been suggested through Ultraviolet-visible spectroscopy, Ft – IR spectra showed the Coordination of the nickel complex with the nitrogen atom from azo group as well the oxygen from the pyrazolone ring hydroxyl groups. A good binding constant of DNA was showed from the binding studies of the metal complexes. To check their serviceability, the chromium complexes were applied on the leather, as well They showed moderate to high values from sweat fastness as well as light fastness and also shades for acid dyes ligand and chromium complex dyes as shown in **Table 1 and Table 2.**

Table 1: Acid dyes ligands fastness properties [6(a-f)] with metal ions complexes [7(a-f)].

Dye	2%Shade on Leather	5%Shade on Leather	Penetration	Washing Fastness	Light Fastness	Perspiration Fastness
6a	Yellowish Orange	Reddish Orange	2	2-3	2-3	3-4
7a	Olive	Dark Olive	5	4-5	5	5
6b	Orange	Yellowish Orange	2	2-3	2-3	3-4
7b	Yellowish Orange	Reddish Brown	3	3-4	3-4	4-5
6c	Yellowish Orange	Yellowish Orange	3	3-4	2-3	3-4
7c	Olive	Dark Olive	5	4-5	5	5
6d	Tan	Yellowish Brown	3	3-4	3-4	3-4
7d	Yellowish Orange	Yellowish Brown	3	3-4	3-4	4-5
6e	Greenish Beige	Reddish Beige	2	2-3	2-3	3-4
7e	Light Olive	Dark Olive	5	4-5	5	5
6f	Golden Yellow	Yellowish Orange	3	3-4	3-4	4-5
7f	Yellowish Orange	Yellowish Orange	4	3-4	3-4	4-5

Table 2: Ligand acid dyes properties [6(a –f)] with metal ions complexes [7-(a-f)].

Dyes		6 a	6b	6 c	6 d	6e	6f
Shades on Leather	2% Shade						
	5% Shade						

Dyes		7 a	7b	7 c	7 d	7e	7f
Shades on Leather	2% Shade						
	5% Shade						

In (2019, Jinan M et al) **[9]** has been synthesized 1-(4-amino-3-(benzo[d]thiazol-2-yldiazenyl) phenyl) ethanone by the reaction of diazonium salt of 2-amino benzothiazole with 4-aminoacetophenone as shown in (**scheme-2**).

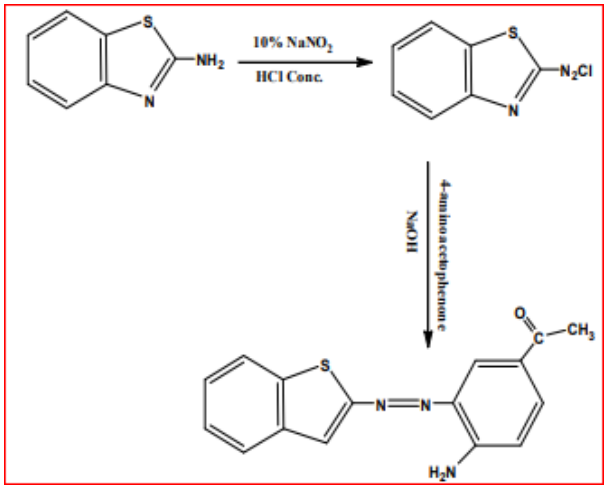

Scheme-2: Preparation steps of primary azo dye ligand.

Metal chelates of (M^{+2} = Co, Ni, Cu, and Zn) were prepared as appear in (**scheme-3**).

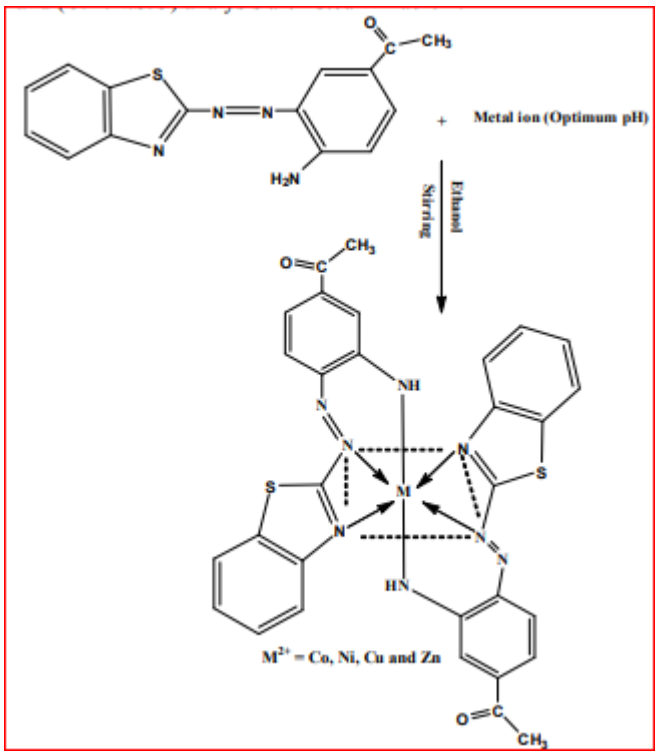

Scheme-3: The suggested structure of azo dye transition metal complexes.

The study of microbial evaluation from heterocyclic spores azo dye ligand name 4-[(5-acetyl-2-aminophenyl)- diazenyl]-1,5-dimethyl-2-phenyl-1*H*-pyrazol-3(2*H*)-one derived for 4-aminoantipyrine as well 4- aminoacetophenone as well their metal ion (II) compounds with some transition metals. The physical properties and the elemental analysis (C, H, H, N, O, S) of the azo dye ligand and its metal complexes, and the magnetic measurements for the complexes with other analytical methods were studied. According to these results of investigations, the octahedral geometry was suggested for all of these complexes**.** The ligand as well as its transition metal (II) complexes possess notable microbial activities. The Incorporation of the azo group into the structures of compounds such as benzimidazoles, azomethines, 2- aminothiazoles, and other benzothiazoles, compounds have a noticeable effect on the biological activity of the compound and its complexes; In fact, the only explanation for why some of the compound's inhibition results are similar to its complexes is that the effect of the heterocyclic compounds with the azo group will reduce their activity against the bacterial cell membrane, in addition to the presence of the effect of the metal ion salt that is coordinated with the ligand, and thus some of the inhibition results of the complexes are equal to the ligand. **[10].**

(In 2019, Virendra R. Mishraa, et al) **[11]** has been used diazo coupling to create an azo-linked substituted benzothiazole, benzoxazole, and benzimidazole, as shown in **scheme -4**.

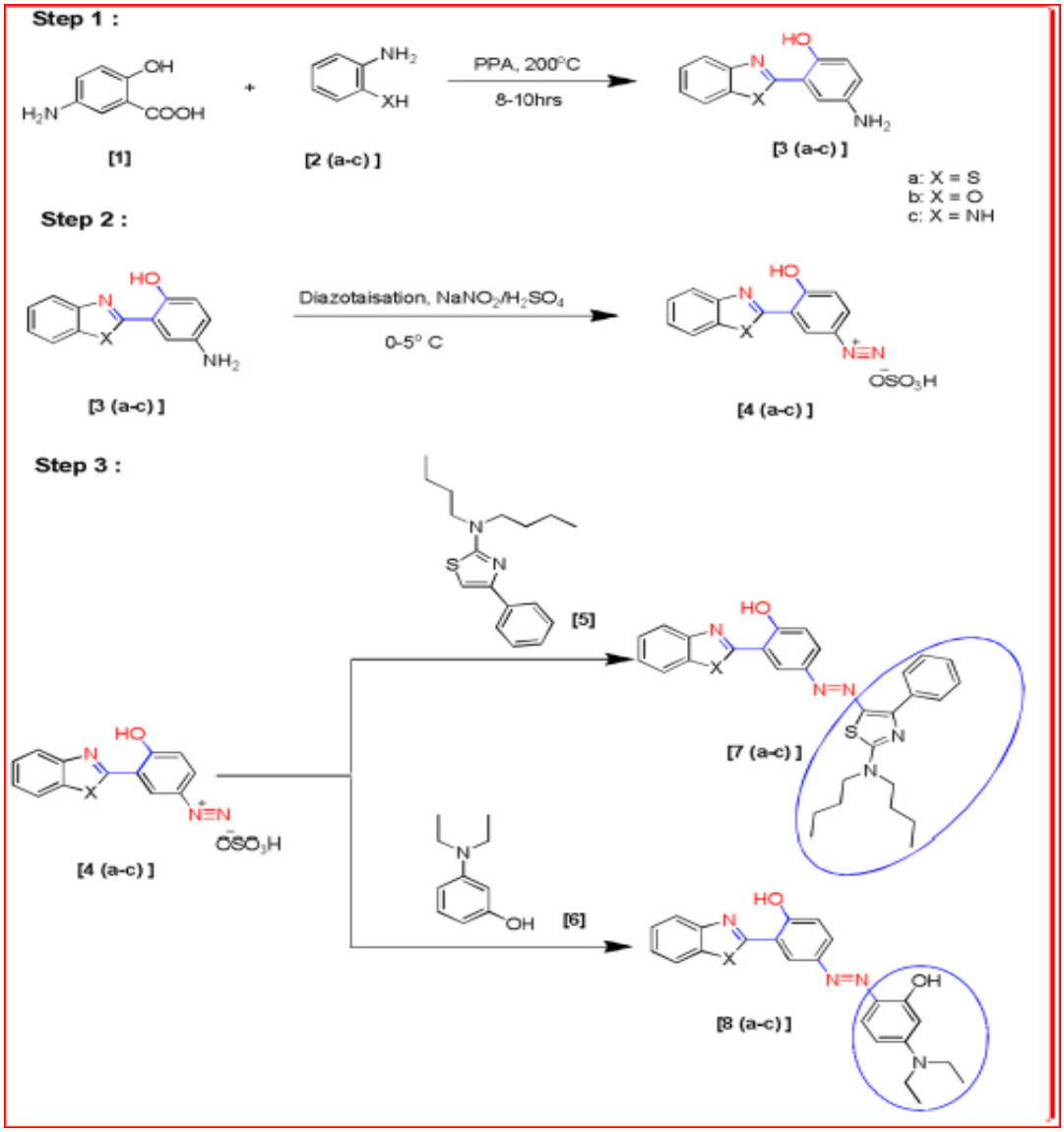

Scheme-4: The preparation, and coupling steps of heterocyclic azo dyes compounds.

These compounds have been then examined using FTIR, elemental analysis, and ^{1}H NMR, as well as Ultraviolet spectroscopy analysis. By using Resazurin Microtiter Assay Method (REMA), newly synthesized compounds have been tested with in vitro anti-bacterial efficiency versus *Staphylococcus aureus* as well *Escherichia coli* strains. The antibacterial activities were expressed as the minimum inhibitory concentration (MIC in g/mL). The anti-bacterial efficiencies for the azo-bound compounds were good to moderate or strong in vitro. The correlation between the HOMO-LUMO gap and anti-bacterial efficiency was studied computationally. Comparative molecular docking studies have provided more useful information about binding mechanisms, Our docking studies also led us to the conclusion that these compounds might develop into anti-microbial agents in the future. In comparison to Ciprofloxacin, comparative docking studies at PDB ids-2XCS as well 1D7U show good anchoring results on common bacterial targets. It was found that 8a has a smaller HOMO-LUMO gap (3.04 eV) than 8b and 8c. Therefore, it ought to have greater biological activity, which is supported by the REMA assay method. However, using the REMA assay method (Resazurin Microtiter Assay Plate method), we found a similar activity for atoms, and it was unrelated to a HOMO-LUMO gap. as shown in **Figure -2.**

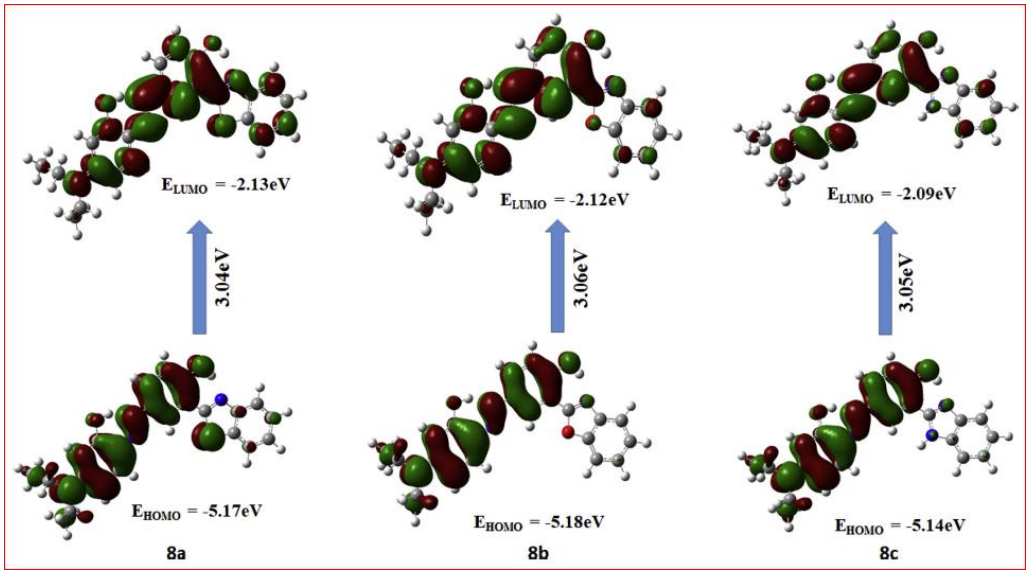

Fig - 2: plot **8(a, b, and c)**, for HOMO-LUMO

(In 2019, Dilek K, et al), **[12]** used an economical chemical precipitation method to create the Schiff base metal complex Zn (II). By using XRD analysis, it was discovered that Schiff base mineral complex Zn (II) has been polycrystalline as well as nano-sized (21.43 nm). In organic dye-sensitive solar cells. This metal compound for a polycrystalline structure has been utilized as a sensitizer. The analysis revealed that these metal complex's power conversion efficiency value was 0.73. Despite having a low solar cell performance, Schiff base mineral complex Zn (II), which can be made using straightforward and inexpensive chemical processes, was found to be very significant while compared into efficiency for expensive organic dyes. The main goal of this research is to determine the power conversion efficiency of Schiff base metal complex Zn (II) that is bound into a 5 amino-2,4-dichlorophenol-3,5-ditertbuthylsalisylaldimine ligand when utilized as a sensitizer in a dye-sensitive solar cell device. The calculated % value of the Zn (II) metal Schiff-base complex was 0.73 as a result of the obtained J-V curve as shown in **Figure -3**. This finding suggests that the Schiff base metal complex Zn (II)is When electron transfer is an important component. As a result, it can be concluded which Schiff base metal complex Zn (II), which can be produced at a low cost, has the potential to serve as a sensitizer for dye-sensitive solar cell technology.

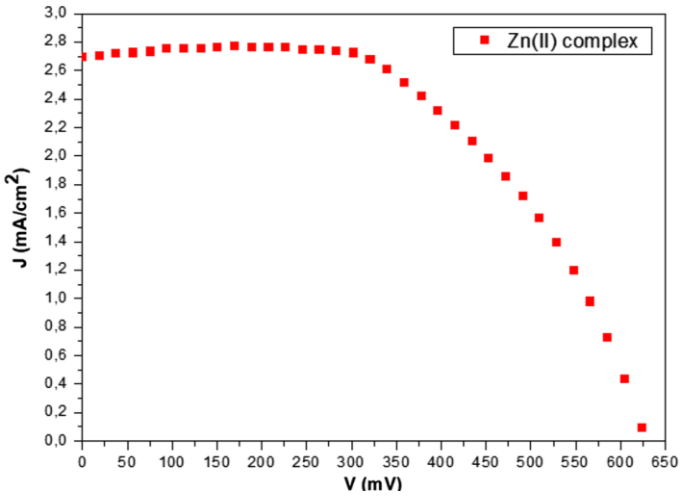

Fig-3:The Zn(II) metal Schiff–base complex with ligands recorded J-V spectrum

(In 2019, Chandana. S, et al), **[13]** note that Quinolinyl-azo-naphthol (HL) exhibits a 750-fold increase in emission on 612 nm when excited in visible light (537 nm), making it a selective turn-on chemo sensor with Al^{3+} at existence from other ions. (LOD: limit of detection for Al^{3+}) in drinking water is 0.69 nM (3σ method), which is significantly less than the (7.41 µ M) WHO recommended value. ESI-MS spectrum data as well as Job's plot both support that the isolated compound $[AlL_2]$ has the structure it does. According to the results of ESI-MS spectra data shows the $[AlL_2]^+$ composition. The probe's mass spectrum exhibits a peak at 322.05 that $[HL]^+$ $Na^+]$ is responsible for. and m/z 300.07 was referred to [HL $^+$ $H^+]$, HRMS ($TOFES^+$): m/z computation. For $C_{19}H_{13}N_3O$ (M+ H+) = 300.11, 300.07 was found., Mp: above 210 C^0. The composition $C_{38}H_{24}AlN_6O$ (cal. 623.17) for $[AlL_2]$ is represented by the strong peak at 623.36. HRMS ($TOFES^+$): m/z computation. AlL^{2+}, = 623.17 for $C_{38}H_{24}AlN_6O_2$, found a value of 623.36. As a result, the mass spectrum is consistent with the formation of an Al^{3+} HL1:2 complex. The complex $[AlL_2]NO_3$ has a melting point above 300 ~C. The emission intensity of the $[AlL_2]^+$ solution is quenched upon the addition from aqueous F^-, as well as LOD from F^- is 0.63 nM. To create portable kits with detection fluoride contamination at drinking water, HL is therefore essential. The probe displays an INHIBIT and azo-hydrazo tautomerization. The outcome of this work was the successful use of a quinoline-azo-naphthol derivative (HL). An incredibly selective fluorescent probe has been manufactured to distinguish Al^{3+} ions from other metal ions When more Al^{3+} is introduced to a clean water medium, this newly created probe, called HL, exhibits a remarkable emission enhancement that causes a redshift of the emission maximum at 612 nm as well as a discernible color change into bright red. as shown in **scheme -5**, and **Figure -4.** Additionally, under physiological conditions, The inclusion of a fluorescent probe demonstrates strong Al^{3+} selectivity at low enough detection limits of 0.69 nM (WHO suggested data, 7.41µM). Luckily, the molecule $[AlL_2]NO_3$ is 104 times more sensitive to F than the 3.9 x 10^{-6} M WHO recommended toxicity limit. Moreover, by monitoring emission mode at 612 nm, HL shows an INHIBIT logic gate for Al^{3+} and F-such as chemical inputs. The $[AlL_2]^+$ complex is used to collect groundwater, and it is extremely effective at detecting the presence of F^-. The azo-hydrazo tautomerization from free HL has been as well studied in methanolic solution as one of the significant chemical phenomena. The experimental results are explained using DFT and TDDFT computation methods.

Scheme-5: Describe how the truth table and circuit employ the emission mode as the output and Al^{3+} and F as the chemical inputs.

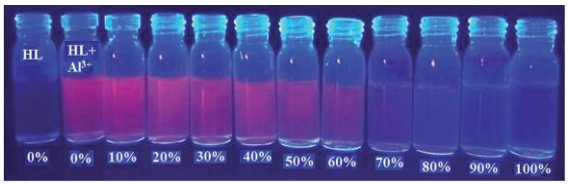

Fig-4: Explain the increase in the amount of F-contaminated water (0–100%) added to the complex solution (HL + Al $^{3+)}$ under UV light causes a visual change. Purulia-I.

(In 2020 Farhana. A, et al) **[14]** The efficient synthesis of palladium nanoparticles for guar gum as a stabilizer as well as their employees such as catalysts with reduction reactions and decomposition from azo dyes is studied. The high cost of the materials is the main barrier to its widespread use. In the current study, a green method of synthesis was used to create a cost-effective palladium nano-catalyst using guar gum such as a capping as well reducing agent. Palladium nanoparticle formations have been verified through UV spectrophotometer, and morphology as well as nature were verified by SEM as well XRD, that demonstrated that PdNPs are crystalline and roughly spherical. Guar gum can both stabilize and reduce Pd (II) to Pd (0), according to FT-IR analysis, which also revealed the various functional groups of reducing agents. The presence of a distinct palladium signal in EDX spectra provided additional evidence that PdNPs had formed. The hydrogenation of 4-nitrophenol was used to examine the catalytic effectiveness. The prepared nanocatalyst's rate constant was 0.1436/min, and its TON (Turnover number) and TOF (Turnover frequency) in the aforementioned reaction are 90.83, 27.78, as well 185.2/ hrs, respectively. Based on the datum, it was determined that synthesized PdNPs were effective heterogeneous catalysts for the azo dye deterioration and the reduction of 4-NP. Further confirmation of the reduction of palladium chloride came from UV spectroscopic analysis between 300 and 700 nm .The colorimetric shift is visible in **Figure- 5.**

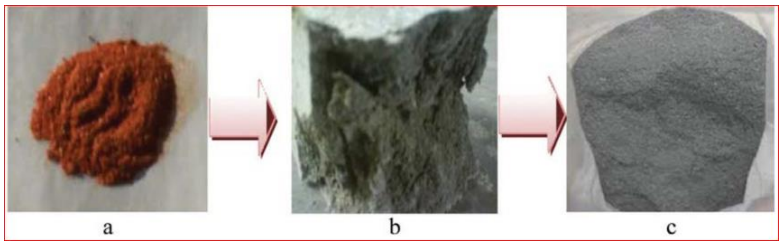

Fig-5: Three examples of **(a)** $PdCl_2$, **(b)** Colloidal PdNPs **(d)** Powdered PdNPs.

The degradation analysis of various dyes was used to evaluate the photocatalytic performance of the PdNPs. The dye solution was supplemented with a known quantity of PdNPs and exposed to

sunlight. 29°C was the average temperature. To achieve absorption equilibrium between the dye as well catalyst before irradiation, the mixture has been stirred at dark with a full hour. To initiate the photodegradation process, a small amount from sodium borohydride reducing agent (1 mL, 10 mM) has been added into the reaction mixture. To track development from the reaction, samples of the dye mixture were taken at predetermined intervals of UV irradiation and the UV spectra were recorded. The repeated cycles of the photo-catalytic experiment were used to look into the stability of the PdNPs.

Methyl orange (MO), methyl blue (MB), as well Congo red (CR) catalytic reduction

The catalytic activity of the prepared PdNPSs was evaluated at a catalytic reduction from MO, MB, as well CR also at a catalytic reduction from a mixture of the three. The UV spectrophotometer was used to track the reaction's development. These result demonstrated how well the prepared PdNPs reduced CR, MB, MO, as well as a mixture from all three dyes when reduced with $NaBH_4$ aqueous solution. Based on the results obtained the Pd nanocatalyst that has been prepared is stable as well can be recovered as well used at least seven additional times to completely reduce organic dyes.

(In 2020 Marwa Ali Dahi, as well Amer J. Jarad) **[15]**. Studied the reaction between 4-methoxy aniline with 2-amino benzothiazole (diazonium salt) to obtain (E)-2-(benzo[d]thiazol-2-yliazenyl)-4-methoxy aniline as shown in **scheme -6**.

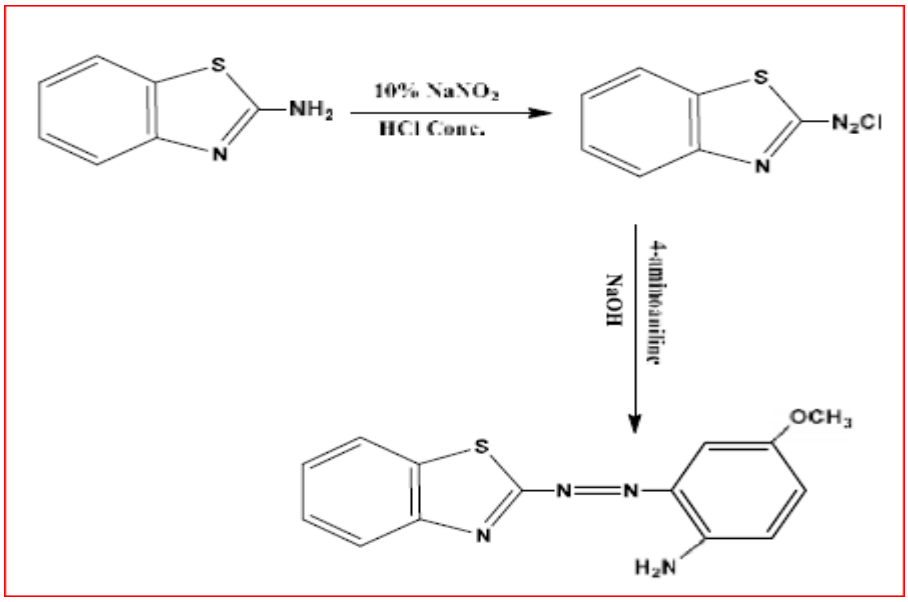

Scheme -6: Steps of preparation of azo dye ligand.

From this ligand new metal complexes of (Co^{2+}, Ni^{2+}, Cu^{2+} and Zn^{2+}) were prepared according to **scheme – 7.**

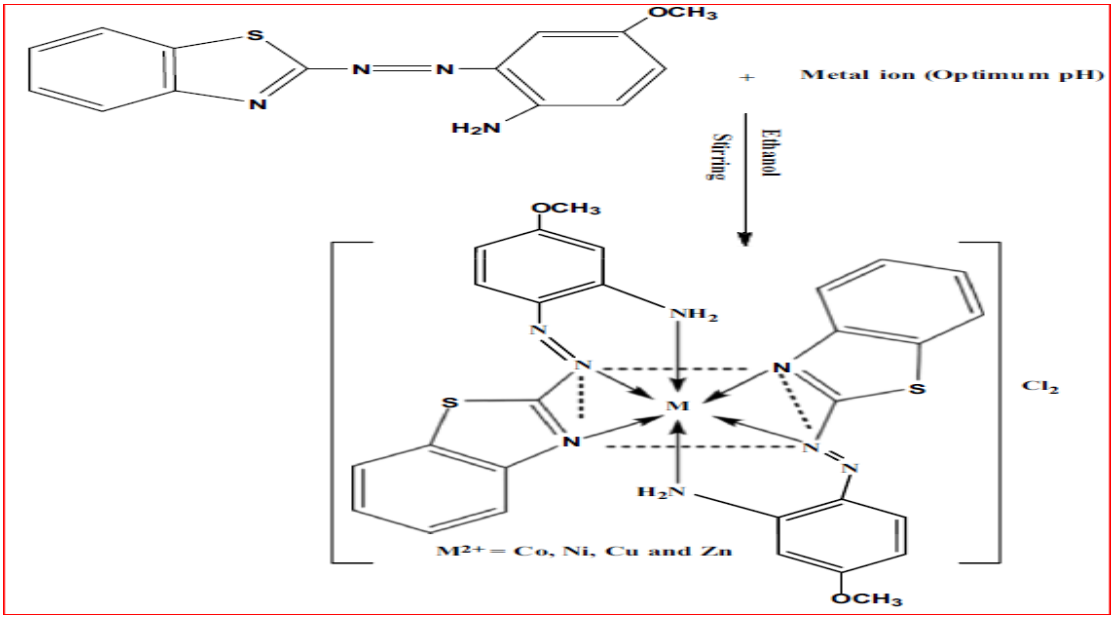

Scheme – 7: Synthesis of metal complexes of azo dye ligand.

The thiazolyl azo ligand and their complexes were characterized by using various techniques such as 1HNMR UV-Vis, FTIR, microanalysis of the elements (C.H.N.S.O). The mechanism of mass fragments is shown in **schemes – (8 and 9)**.

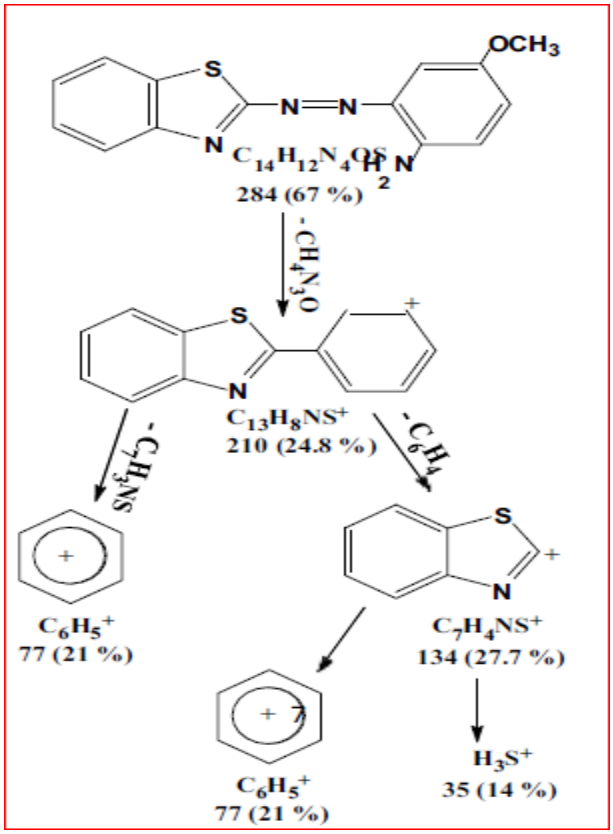

Scheme -8: Mass fragments mechanism of azo ligand

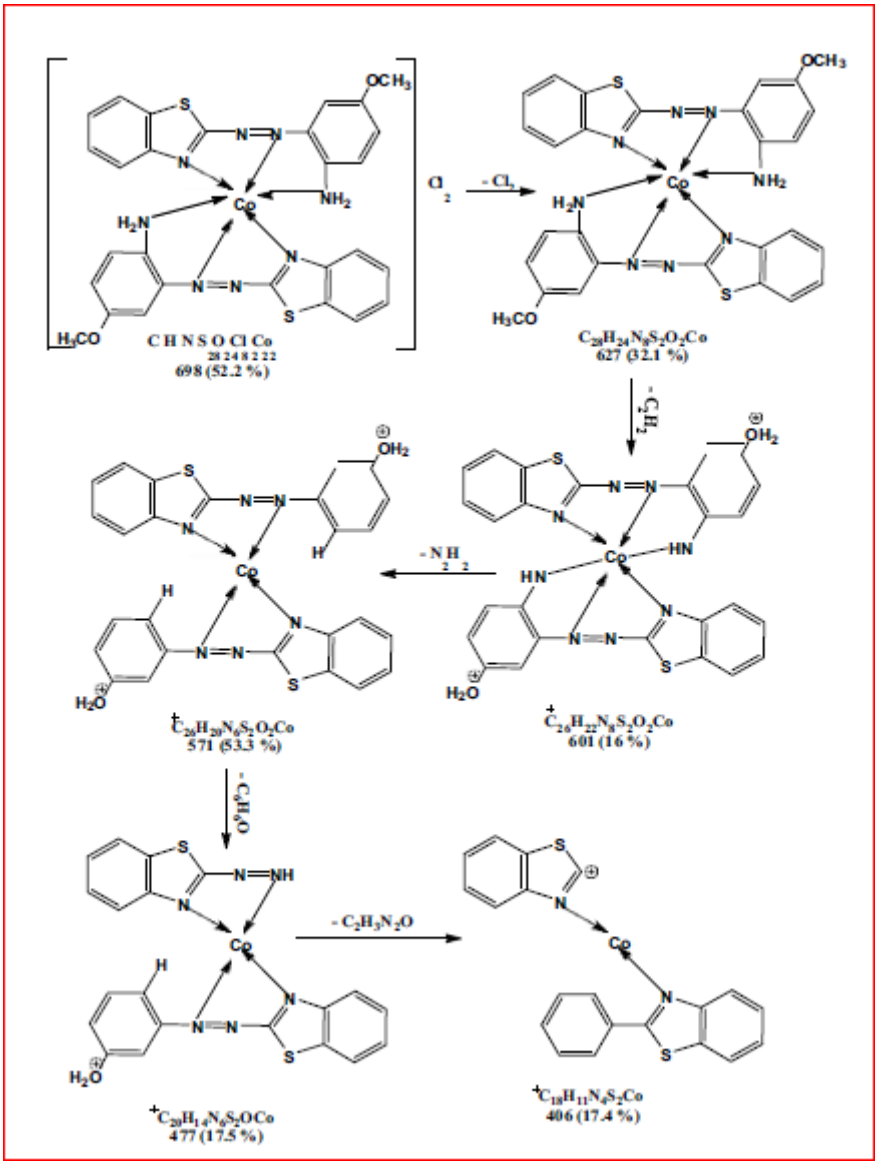

Scheme – 9: Mass fragments mechanism of Cobalt complex.

Other techniques like atomic absorption of flame, also electrical conductivity as well magnetic quantities for complexes and conditions reaction were appeared studied. The nature of the compounds formed was studied using (mole ratio and continuous contrast) methods, with Beer's law ($1x10^{-4}$-$3x10^{-4}$ mole/L) applied during the concentration scope. Compound solution height molar absorptivity has been observed. The complexes all had a metal-to-ligand ratio of 1:2. The main purpose of this work is to synthesize, some metal complexes containing the thiazolyl azo dye that have been designated as chelating ligands. Additionally, studies of the biological activity of all produced compounds were evaluated against different anti-microbial strains. The Ligand (L) and its complexes' biological activity results revealed the bacteria's inhibition circle diameter in millimeters after 24 hours.

(In 2020 Shatha M H Obaida et, al) **[16]**. Azo ligand (4-chloro-N-(2-(dimethylamino)ethyl)-5-((2-hydroxy-4,6-dimethylphenol)diazenyl)-2- methoxybenzamide) L . **scheme -10**.

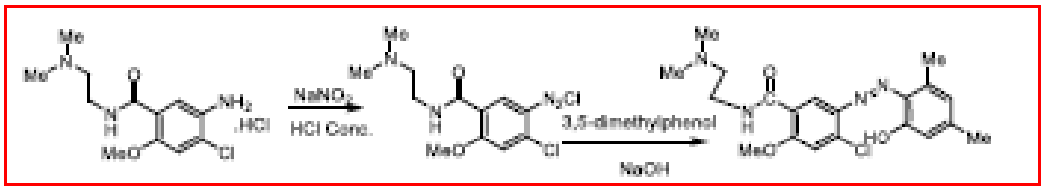

Scheme – 10: Synthesis of azo ligand.

This ligand was used to form four complexes of Co (II), Ni (II), Cu (II), and Zn (II) as shown in **scheme-11**.

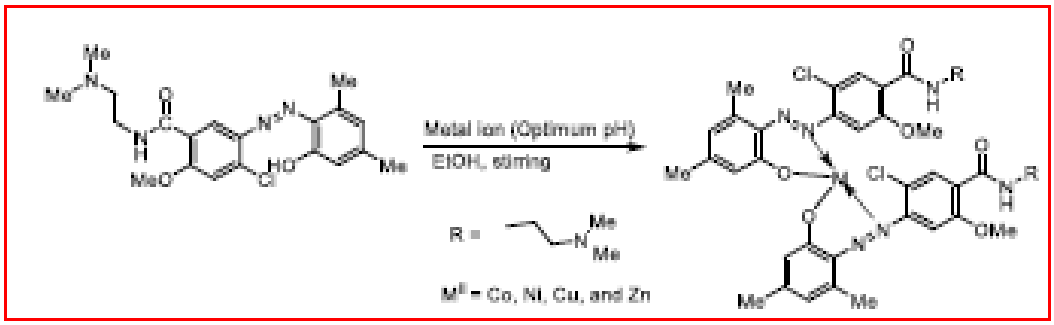

Scheme – 11: Synthesis of metal azo ligand complexes.

The physical properties of the azo ligand and its metal complexes were studied. Azo ligand and Nickel complex mechanism fragments were explained briefly in **schemes -12,** and **13.**

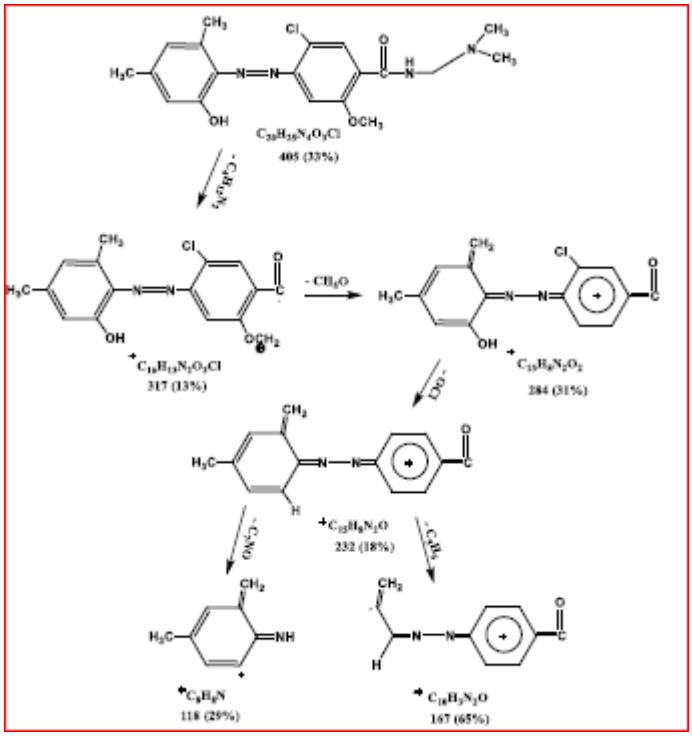

Scheme – 12: Mass mechanism fragments of azo ligand.

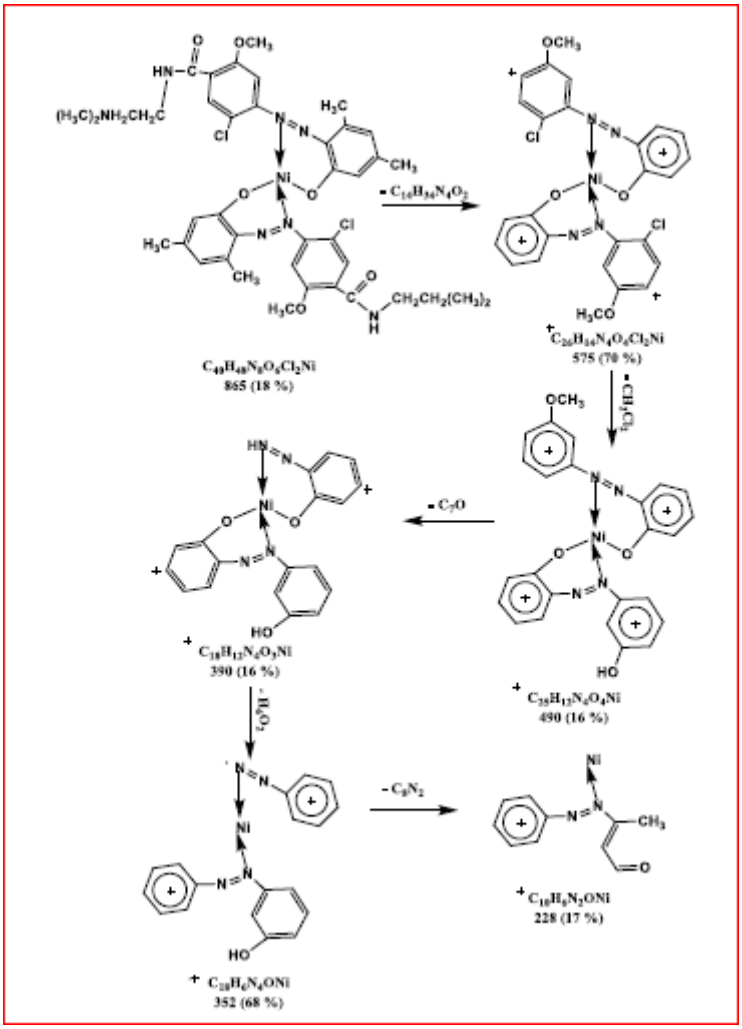

Scheme – 13: Mass mechanism fragments of Nickel complex.

These dyes were evaluated for their ability to dye cotton cloth, as well as for light and cleaner firmness. Based on their analytical and spectroscopic data, the structure of the ligand and complexes was verified. The ZnL compound demonstrated greater anti-bacterial efficiency with an inhibition zone of 13 mm against *Staphylococcus epidermidis*, *Streptococcus sp.*, and *Escherichia coli* compared to the ligand and other metal complexes, according to an evaluation of the anti-microbial and anti-fungal efficiencies of ligand and their complexes. There is no question that the antifungal activity of Candida albicans showed higher inhibition in the case of the ZnL compound, with a 15mm inhibition area showing higher efficiency for ligands as well as other metal complexes. Anti-microbial effectiveness research has been published in opposition to the tested organism as shown in **Figure 6**.

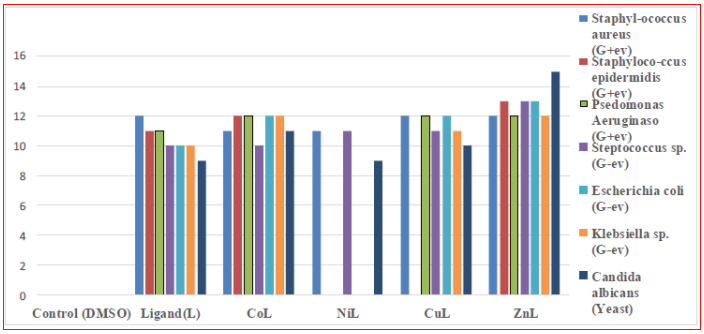

Fig – 6: An illustration of the ligand and its complexes' antibacterial and antifungal activity that measures the inhibition zone (mm). Dimethyl sulfoxide.

Dye and its generated compounds were applied to cotton fabric based on the results of a tetrahedral structure that was postulated using manufactured compounds.as shown in **Figure -7**.

Fig – 7: The textiles, dyeing sample, and their metal chelates comprise the ligand (L).

(In 2021 Isaac O. A, et al) **[17]** ethyl-4-((4-chlorophenyl) carbamoyl) was created.5-methylthiophene-3-carboxylate and ethyl-2-((5-cyano-1-ethyl-2-hydroxy-4-methyl-6-oxo-1,6-dihydropyridin-3-yl)diazenyl)-4-(carbamoyl)(4-chlorophenyl)5-methylthiophene-3-carboxylate -2-((5-cyano-2-hydroxy-1,4-dimethyl-6-oxo-1,6-dihydro-pyridin-3-yl) diazenyl). A coupling reaction between synthesized ethyl 2-amino-4-((4-chlorophenyl) carbamoyl) and other compounds produced these dyes.5-methylthiophene-3-carboxylate reacts with 6-hydroxy-1,4-dimethyl-2-oxo-1,2-dihydropyridine-3-carbonitrile and 1-ethyl-6-hydroxy-4-methyl-2-oxo-1,2-dihydropyridine-3-carbonitrile. The synthesized dispersed dyes underwent metal complexation with copper, cobalt, and zinc metals, as shown in **scheme -14**.

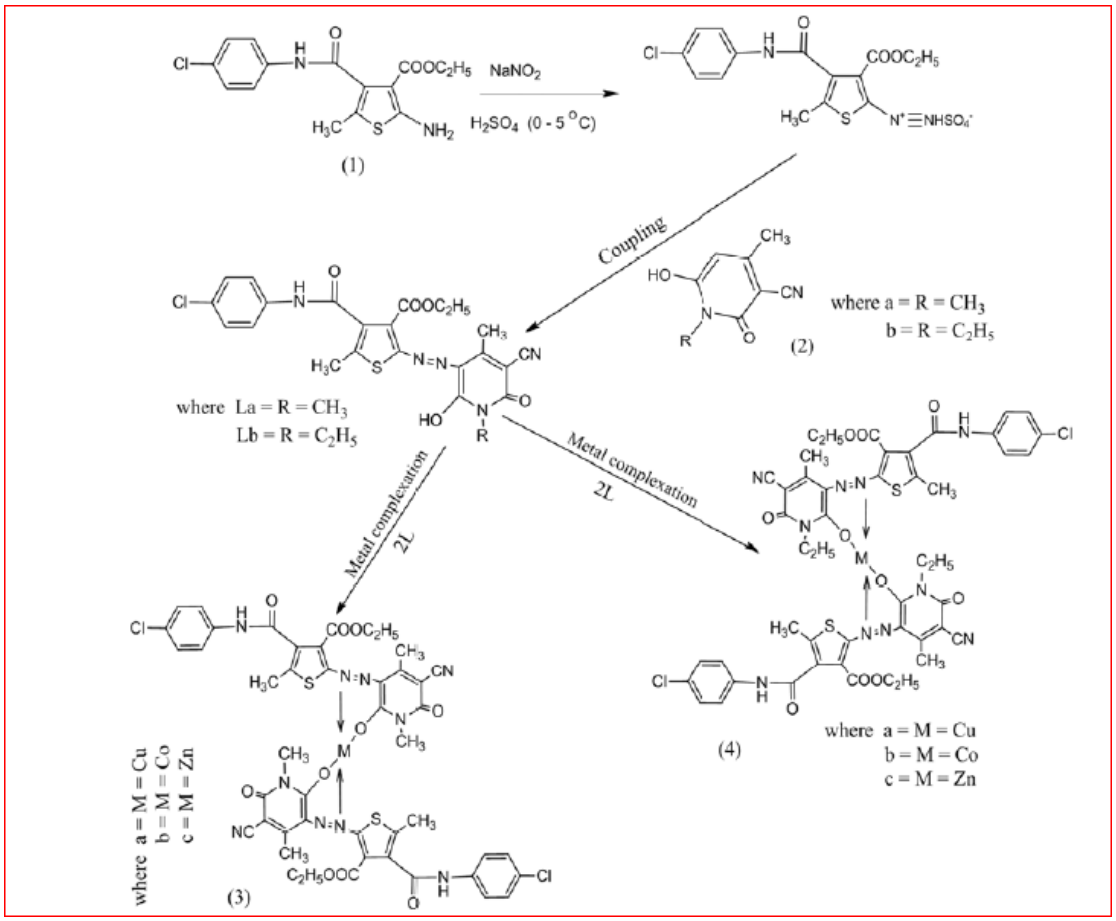

Scheme – 14: Synthesis steps of azo dye ligand and metal complexes.

These compounds are investigated using analytical methods like proton nuclear magnetic resonance (1H NMR), carbon- 13 nuclear magnetic resonance (^{13}C NMR), and mass spectrometry (MS), Fourier transform infrared (FTIR), ultraviolet-visible spectroscopy, and the determination of their melting points, the structure of the synthesized intermediate, coupling components, dyes, as well complexes have been clarified. Dyes' as well as complexes' molar extinction coefficients range from 24,800 to 83,200 $Lmol^{-1}cm^{-1}$. FTIR spectra of these dyes and their complexes revealed the presence of cyano, carbonyl, hydroxyl, and azo groups in the ranges of 2225 to 2229 cm^{-1}, 1640 to 1692 cm^{-1}, 1398 to 1491 cm^{-1}, and 3474 to 3478 cm^{-1}, as well as aromatic (C-H) and (N-H) stretching vibrations in the 2882–2989 cm-1 range. The dyeing properties of the dyes and metal complex analogs have been assessed using polyester and nylon 6.6 fabrics. It was found that the dyes and complexes have good to excellent wash fastness, light fastness, good to exceptional fastness to perspiration and sublimation, and good levelness on both polyester and nylon 6.6 materials with varying hues of brown and violet. The shades of Nylon 6.6 and Polyester are depicted in **Figure -8.**

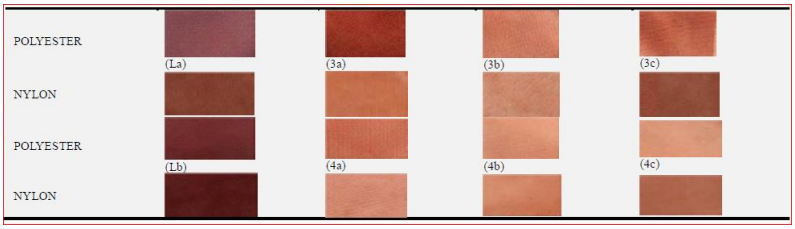

Fig-8: The shades of Nylon 6.6 and Polyester.

The outcome of this study is, that synthesized intermediates, coupling elements, dyes, and their metal complexes had good yields between 63 and 99%. Following application of dyes as well complexes to polyester and nylon 6.6 fabrics, The polyester fabric had outstanding (5) fastness to perspiration and sublimation, while the nylon 6.6 fabric had very good (4) to excellent (5) fastness. This might be explained by the crystalline structure of the polyester, which stopped the color from leaving the fabric after it had entered it. Furthermore, it was shown that polyester nylon 6.6 exhibits good stability in both light and wash conditions. The dyes and complexes derived from the aminothiophene intermediate employed in this study have the potential to be used to color most hydrophobic fibers because of their good application capabilities.

(In 2021 Abaas O. H, et al) **[18]** With the help of 2,4-dimethylphenol and 4-aminobenzoic acid, the azo ligand 4-((2-hydroxy-3,5-dimethylphenyl) diazenyl) benzoic acid and their complexes were synthesized as shown in **schemes 15, and 16**.

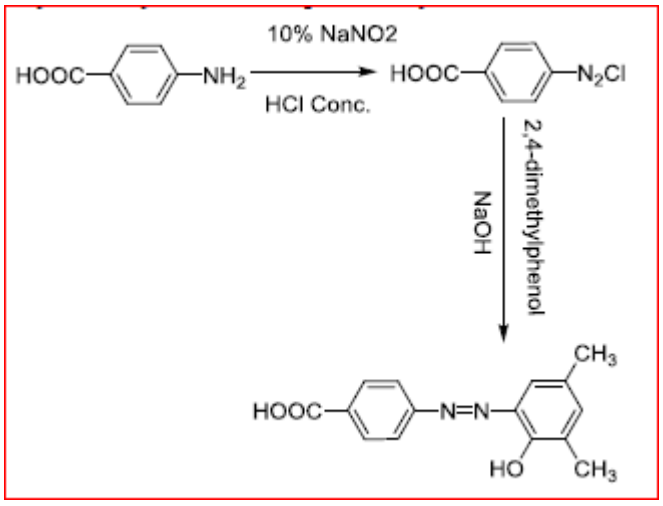

Scheme – 15: Preparation steps of azo dye ligand.

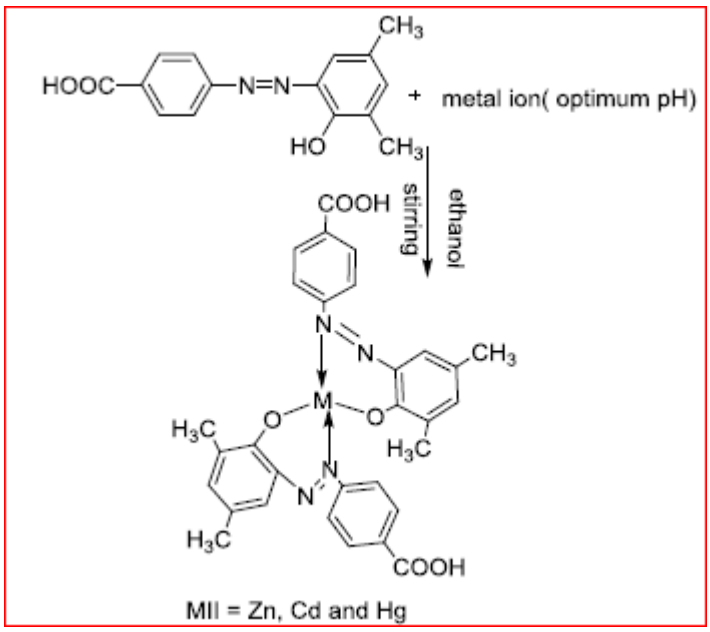

Scheme – 16: Preparation steps of azo dye metal complexes.

Various methods (1H-NMR, UV-Vis, and FT-IR) have been used to characterize azo dye compounds. With the help of the azo ligand (L), metal chelates of (Cd II, Hg II, and Zn II) have been created. Conductivity, elemental analysis (C.H.N.), and spectral studies have all been used to identify the compounds that have been produced. Produced metal chelates were examined using mole ratios and contrast types of sequences. Beer's law applies to the rate of concentration ($1x10^{4}$-$3x10^{-4}$ Mole/L). Molar absorptivity has been observed in compound solutions, these analytical data support the formation of azo ligand and its complexes. The application of ligand and compounds as dispersed colors on cotton fabrics allowed researchers to examine the antibacterial activity of the generated compounds against a variety of bacteria and fungi. as shown in **Figure -9.** Each primed complex has a suggested tetrahedral geometrical structure for the gained datum.

Fig-9: Examples of azo ligand and metal chelates textiles dyeing.

(In 2022 Eman H. Sahap, et al) **[19]** An unpretentious hydrothermal method was used to prepare titanium dioxide (TiO_2) at 180°C for 4 hours. TiO_2 was examined using x-ray diffraction spectroscopy, transmission electron microscopy (TEM), field emission scanning electron microscopy (FE-SEM), as well ultraviolet-visible spectroscopy. This work illustrates the development of complex Ni-azo dye and azo ligand-based TiO_2 thin-film dye-sensitized solar cells (DSSCs). Azo ligand as well the complex Ni (II) as shown in **scheme -17** and **Figure- 10**.

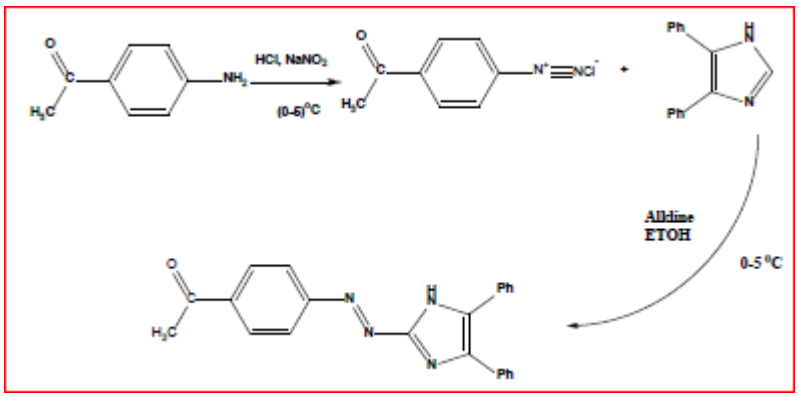

Scheme-17: Synthesis steps of the azo ligand.

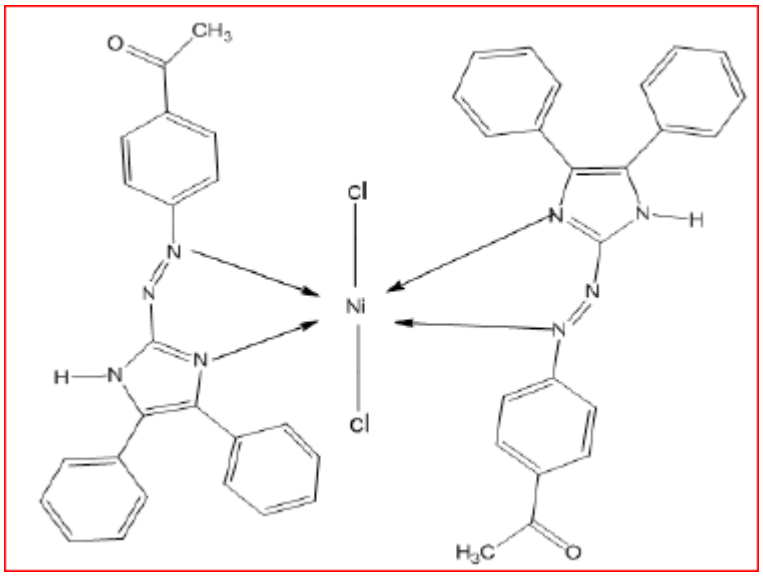

Fig-10: (4-ACPI) with Ni (II) complex.

The ligand and Ni (II) complex was identified by using spectroscopic studies in neutralization, including Fourier transform infrared spectroscopy (FTIR), ultraviolet-visible (UV-vis), as well proton nuclear magnetic resonance (1H-NMR). Under 100 mW/cm^2 standard visible light, current-voltage (I-V) characteristics demonstrate that the DSSCs have a higher change efficiency for TiO_2/Ni-azo dye than TiO_2/azo dye, at about 2.30% and 1.88%, respectively. The structural, morphological, and optical properties of the synthesized NiL_2Cl_2 and $C_{23}H_{18}N_4O$ azo dye were examined using photovoltaic parameters derived from the I-V curve, respectively. As a result, DSSCs can be applied with NiL_2Cl_2 and $C_{23}H_{18}N_4O$ azo dyes as an appropriate sensitizer. **Figure 11**, showed that, For the two dye-sensitive solar cells, I-V measurements were compared: TiO_2 and Ni-Azo dye[(A)Voc = 0.690v], [Jsc = 5.333mA / cm^2], [FF = 0.612, and % = 2.30] [(B) Voc = 0.650V],[Jsc = 4.766mA/cm^2], [FF = 0.256, and % = 1.88%]for TiO_2 and Azo dye.

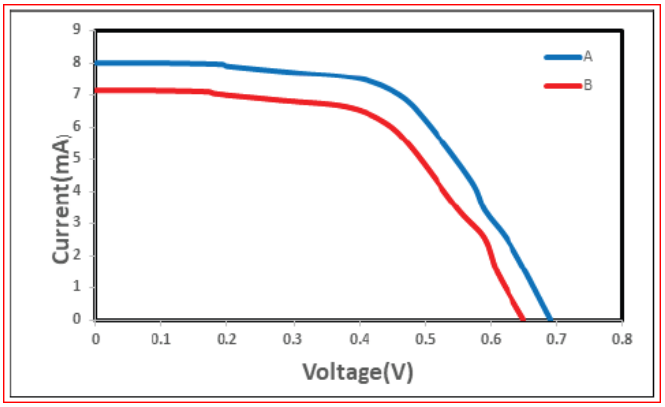

Fig-11: I-V curve measurements were made for the two dye-sensitized

solar cells: (A) TiO2/Ni-Azo dye in comparison to (B) TiO_2/Azo dye.

(In 2022 Anh Van Nguyen, et al) **[20]**, isolated ten metal complexes for Cd (II), Zn (II), Ni (II), Cu (II), and Co (II), two novel azo-colorants derived from phloroglucinol and antipyrine and also investigated using a variety of techniques (^{1}H, ^{13}C NMR, IR, UV -vis, EPR, and X-ray structure determination). Phloroglucinol was azo-coupled for a 5-pyrazolone amino-derivative to produce colorant H_3L_1, which has been found to exist at hydroxy-azo tautomeric form as shown in **scheme -18**.

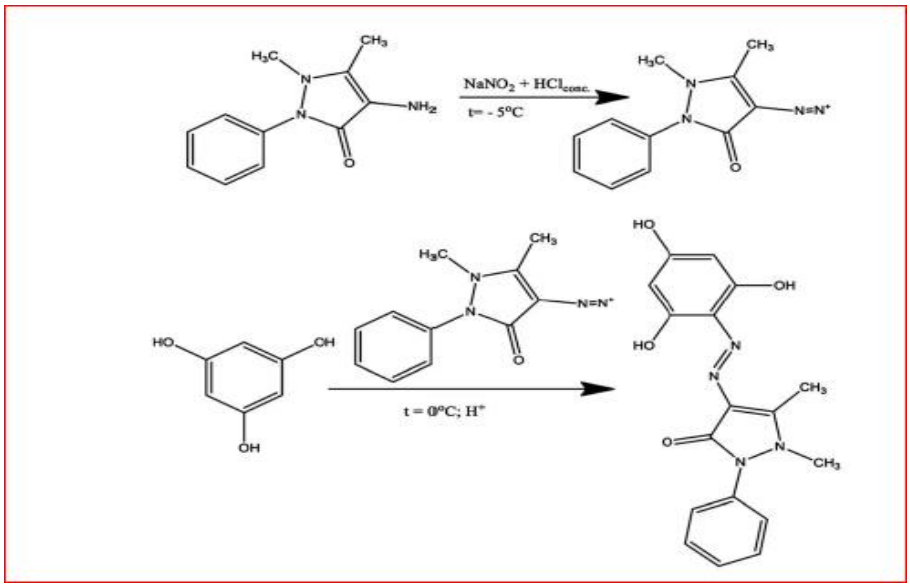

Scheme -18: Synthesis steps of H_3L^1.

Upon nitrosation from H_3L_1, trioxo di-hydroxylamine hydrazone, also known as H_3L_2, was produced as shown in **scheme -19.**

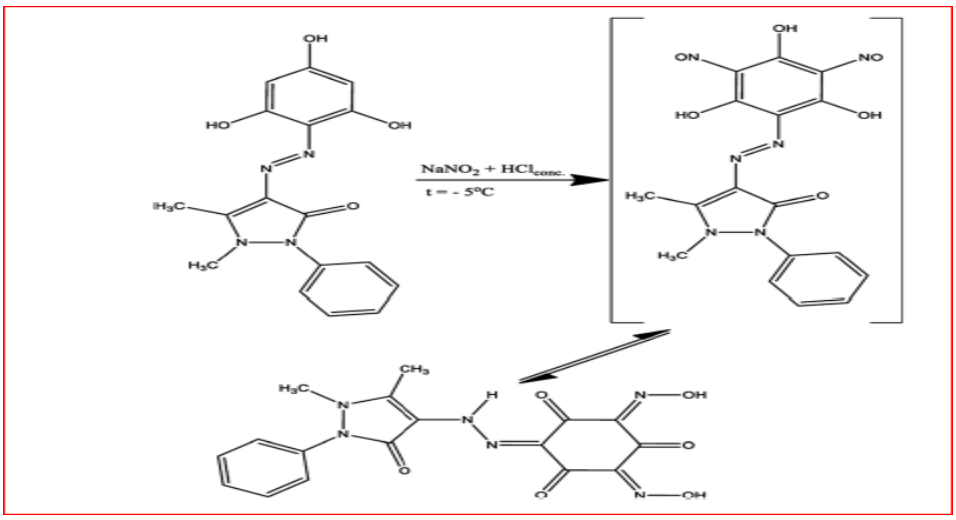

Scheme – 19: Synthesis steps of H_3L^2.

Cd -complex from H_3L_1 displays a dimer conformation from two organic bonds united at the inner domain, as determined through X-ray structure. Formation from dimers between cadmium cations through chloride anions has also been detected. EPR spectra revealed a distorted tetragonal symmetry at the CufH_3L_1 complex that was bound into the dx_2y_2 ground state instead of the dz2 ground state, as well the corresponding Cu-H_3L_2 complex has been also described through cubic symmetry from the coordination medium. All Complexes of H_3L^1 and H_3L^2 are depicted in **scheme – 20**.

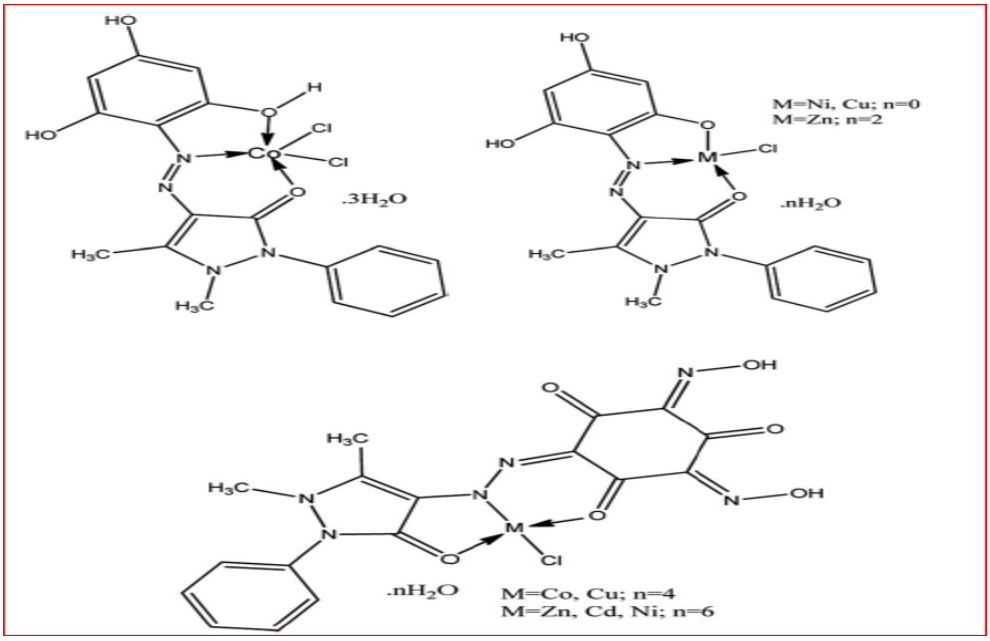

Scheme – 20: Formation of metal complexes of the ligands H_3L^1, H_3L^2.

H_3L_1 as well H_3L_2 as well as mineral complexes show color efficiency toward UV-resistant fibers such as wool, polyamide also polyacetate. Under static as well dynamic conditions, H_3L_2 showed good adsorption efficiency toward heavy metal cations for aqueous solutions from trace concentrations. Wool, polyamide as well polyacetate fibers respond into chromogenic efficiency exhibited through H_3L_1, H_3L_2 as well as mineral complexes. Mineral complexes as well application

properties from ligands have been evaluated, like rubber fastness, washing fastness, and light fastness as well ability to act as wood dyes. Results showed that H_3L_2-colored textiles have been resistant to solutions containing metals, and H_3L_1-colored textiles have been strongly removed from fabric through washing at solutions containing metal cations.

The removal ratio of metal ions rises according to the order $Cu^{2+} > Cd^{2+} > Ni^{2+} > Co^{2+} > Zn^{2+}$ (82-99% respectively). The rate at which metal ions are removed accelerates as pH rises. At pH 5–6, 99% removal of Cu^{2+} ions from the solution is seen to be the most effective. After three cycles of treatment, the removal efficiency of Cu^{2+} cations under a dynamic regime reaches its maximum (the remaining Cu^{2+} condensation is 0.56 ppm, with a 99% elimination rate. Using F-AAS, or atomic absorption spectroscopy

, it was possible to determine initial and residual condensation from metal cations, until three measurements were obtained with a 1% or less difference between them, and the procedure was repeated. All these results are presented in **Figures –12,13,** and 14**.**

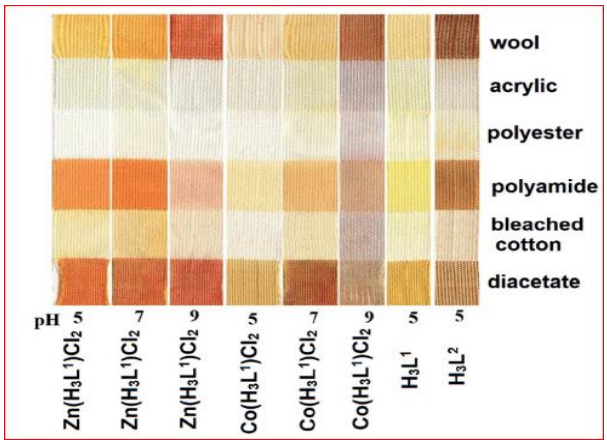

Fig – 12: The test of coloristic for H_3L_1 and H_3L_2 complexes.

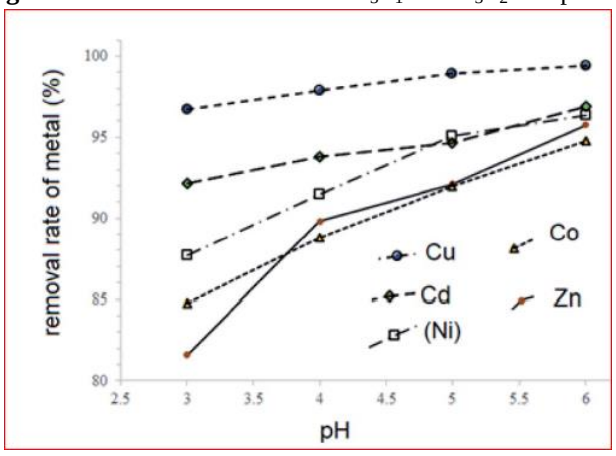

Fig – 13: The pH level effects on H_3L_2's ability to effectively treat solutions containing $CuCl_2$, $CdCl_2$, $CoCl_2$, $ZnCl_2$, and $NiCl_2$ under static conditions.

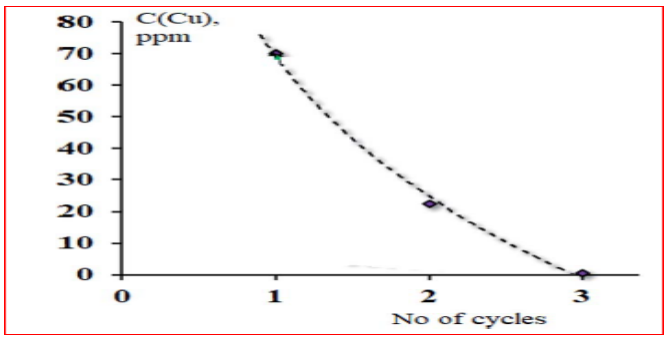

Fig – 14: The effects of several treatment cycles on the ability of wool fibers colored by H_3L_2 to sorption $CuCl_2$ solution under dynamic circumstances.

(In 2023 Adhraa G. A. and Abbas A.S) **[21]** Studied the reaction of 2-hydroxy quinolin derivative, and (HL) : ([4-((2-hydroxyquinolin-3-yl) diazenyl) -N-(5-methylisoxazol-3yl) benzenesulfonamide]) for the following metal ions to form stable complexes for distinctive geometries, like (tetrahedral for both Cu (II) as well Co(II), also (octahedral) with both (Fe (III) also Cr (III))as shown in **scheme-21**.

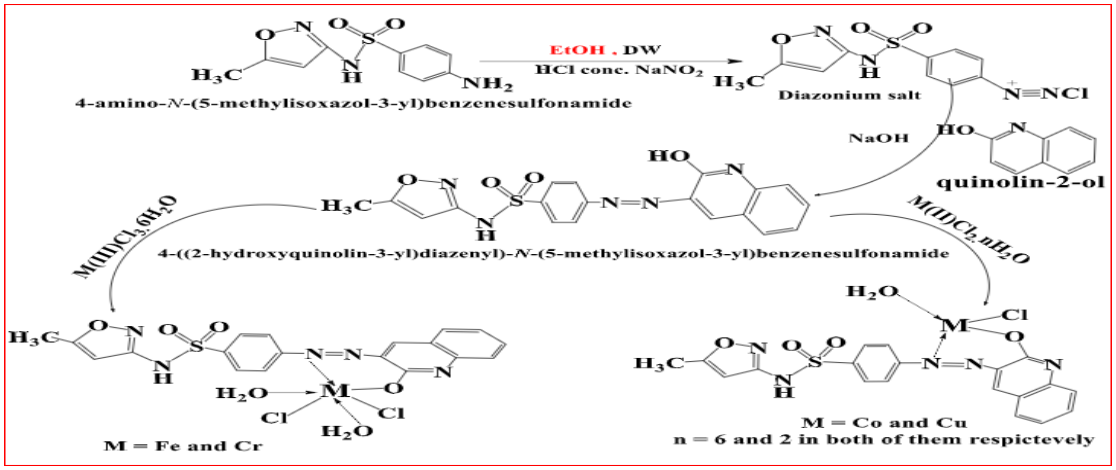

Scheme-21: Formation steps of azo ligand HL and their metal complexes.

Utilizing spectroscopic techniques involving ultraviolet-visible light, which demonstrated the obtained geometries, it was possible to detect the formation of such complexes. Coordination from water molecules for metal ions in the coordination sphere also chlorine atoms was demonstrated by TGA and DSC studies and Fourier transfer in all complexes other than those formed during pyrolysis. Additionally, element-micro-analysis and AAS produced results that corresponded to theoretically /254calculated results. The specific geometries of complexes are also indicated by a magnetic quantification scan. In addition to the results from other techniques, the spectroscopic techniques demonstrated the complex structures, the presence of coordinated water molecules at complexes as shown by the bands at (FT-IR) of the complexes and the degradation processes observed during thermal analysis. The results of the fundamental microanalysis and the experimental incomes were remarkably similar to the calculated incomes. LC-The -NO moiety in Mss data reveals the complexation.

(In 2023, Hoda A. El-Ghamry, et al) **[22]**, Studied the obtained azo bond through coupling diazonium sulfafurazole chloride for resorcinol was designed also synthesized (H_3PIBS: 4-(2,4-Dihydroxy-phenylazo)-N-(3,4-dimethyl-isoxazol-5-yI)-benzenesulfonamide. as shown in **Figure - 15**.

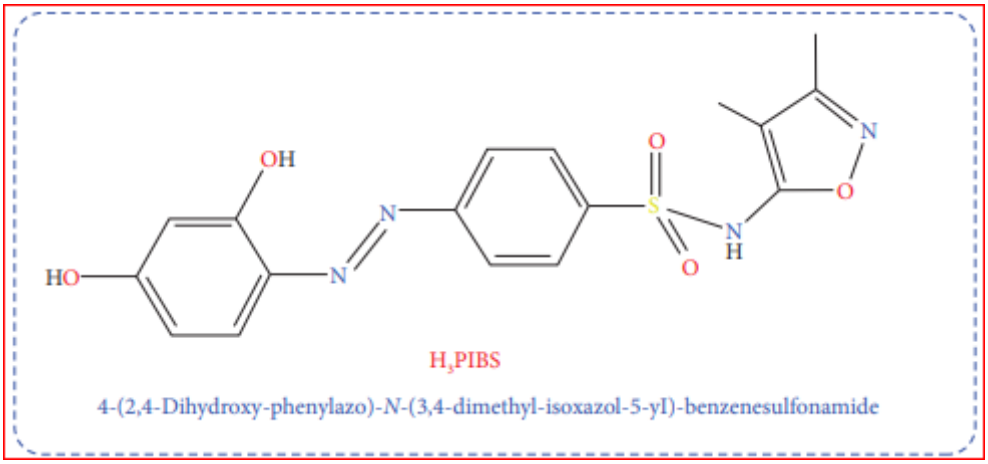

Fig – 15: The Abbreviation and structure of the ligand H_3PIBS

The ligand H_3PIBS and its complexes**.**

A number from divalent as well one trivalent metal chelates. Achieving formation from metal chelates at [molar ratio] from [1L:1M] with Co(II), Fe(III), also Ni(II) chelates while achieving formation from Cu(II) as well Zn(II) complexes at a ratio from 2L:1M allowed with structure investigation from isolated chelates. According to UV-Vis spectra, all metal chelates have an octahedral geometric arrangement around the metal centers. Azo group nitrogen as well the o-hydroxyl oxygen at the ligand were used to attach into metal ions through proton displacement, which caused the ligand to be at monobasic bidentate binding mode. At a trial to ascertain the extent of their efficiency beyond docking studies, the interested compounds' antimicrobial and antitumor activities were assessed versus alternative micro-organisms as well as cancer cells, respectively. UV. Vis spectra also viscosity studies were utilized to examine how the compounds interact with SS-DNA.

Simulation of Molecular Docking:

Most industrial drug discovery programs must include structure-based drug designs. Therefore, interactions between the synthesized compounds and examples of fungal strains, including the *Staphylococcus aureus* adhesion protein receptor (PDB ID: 4m01), were examined to ascertain the compounds' level of biological efficacy first. **Figures 16 (a and b)** show an example of the full profile of interactions between the investigated substances and 4m01. **[23].**

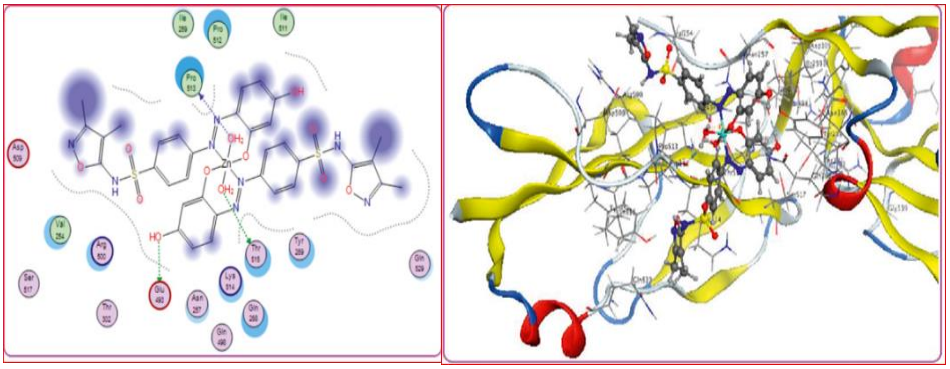

(a) **(b)**

Fig – 16: interactions between H_2PIBS-Zn and the adhesion protein of Staphylococcus aureus in **(a)** 2D and **(b)** 3D.

In addition, the interaction between the compounds under investigation and caspase-3 (PDB ID: 2XYG) is assessed to ascertain the degree of anti-tumor efficacy from the compounds under investigation, as shown in **Figures 17 (a and b)**. The values of the docking score are found to fall between 5.7176 and 7.7365 kcal/mol. H_2PIBS-Cu complex provided the strongest binding, H_2PIBS-Zn complex came in second with a docking score of 7.6576 kcal/mol, after having a score of 7.7365 kcal/mol. Tested compounds' capacity to bind to 2XYG follows the following order (based on the docking score value): H_2PIBS-Cu > H_2PIBS-Zn > H_2PIBS-Fe > H_2PIBS-Ni > H_2PIBS-Co > H_3PIBS.

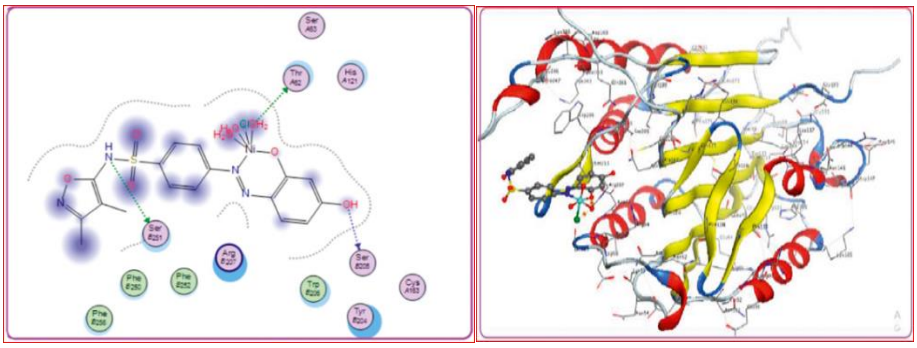

(a) **(b)**

Fig-17: H_2PIBS-Ni and caspase-3 interactions during **(a)** 2D and **(b)** 3D binding.

By docking the co-crystallized ligand of 4ynt, the docking software utilized in the current investigation has been confirmed. The optimal location was chosen and aligned with the docked pose of the same ligand to have the best binding energy, ligand-receptor interactions, and active site residues. With the docking program in operation, the RMSD was 1.546, suggesting good.**[24]**.

Screening with Anti-bacterial and Anti-fungal efficacies:

The good diffusion method **[25]** was used to test the free ligands also complexes under consideration with their anti-bacterial and anti-fungal efficacies, as stated in Supplementary Material. A selected species displays a range of micro-organisms, containing Gram-positive also

Gram-negative bacteria, unicellular and multicellular fungi, and more **[26].** Metal ions, which are more sensitive to microbial cells than organic chelating agents, are typically responsible for the enhanced anti-microbial impact of chelation.**[27].** The stronger influences from mineral chelators may be due to increased lipophilicity in the complexation period. Coordinated metal ions may cause harmful interactions between cellular components or inhibit the activity of cellular enzymes. Evident changes in the activity of various complexes across different organisms are brought on by either variation in the ribosomes in microbial cells or the impermeability of the cells of microorganisms **[28,29].** The ligands examined with their complexes show great promise as novel, incredibly powerful, and broad-spectrum bactericides and fungicides, according to information available in the current research.

Evaluation of Antitumor Activity:

The arsenal of cytotoxic substances currently contains a sizable number of metal-based complexes. In therapeutic contexts, platinum (II) complexes are widely employed, particularly those that target genomic DNA, such as oxaliplatin, carboplatin, and cisplatin. One platinum medication, either alone or in combination, is given to about 50% of cancer patients undergoing chemotherapy. Despite their importance in cancer chemotherapy, platinum drugs have several disadvantages, including dose-related systemic toxicity, a narrow range of antitumor efficacy, moreover, the propensity to result in medication resistance, which typically signifies the failure of treatment **[30].** There is great interest at studying drugs based on non-platinum metals, which are considered effective alternatives in response to observations **[31].** To address this issue, the ability of new compounds to halt, the growth of human cell lines for lung cancer (A-549) and pancreatic cancer (Panc-1) was assessed. The growth inhibitory condensation (IC50) value, which indicates the concentration of the desired substances that, after incubation for 72 hours, results in cell growth inhibition of around 50% as compared to untreated controls, was used to depict the cytotoxicity results. Plotting the cancer cell line survival curve between condensation and cell survival allows one to get the IC50 values. The findings of comparing the IC50 concentrations of synthetic substances with vinblastine sulfate (VS), a commonly used anti-cancer medication, are shown in **Figure 18**. IC50 values for pancreatic and lung cancer cells were 4.68 and 24.6 g/mL, respectively. Different concentrations of each test drug (1.56, 3.125, 6.25, 12.5, 25, 50, and 100 g/mL) were used to dilute it.

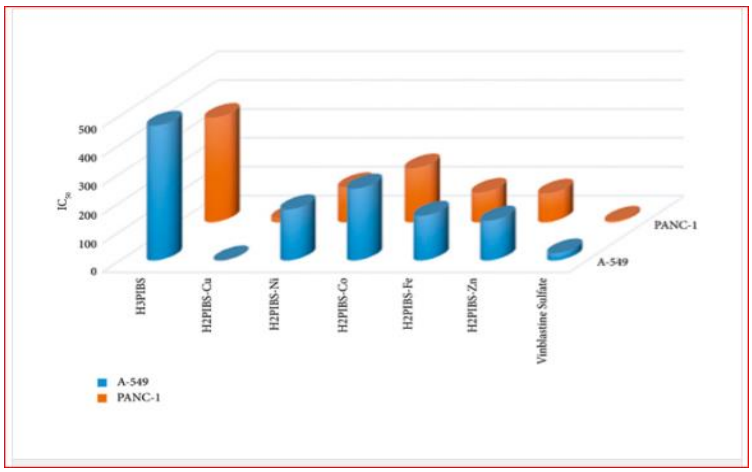

Fig – 18: The values IC50 (g/ml) for H_3PIBS and its metal chelates' in vitro antitumor activity against the cancer cells A-549 and PANC-1.

Each data point represented the average from three different studies using untreated cells as the control also has been expressed such as the value SD**.** ligand H3PIBS, H_2PIBS-Co, H_2PIBS-Ni, H_2PIBS-Fe, H_2PIBS-Zn, and H_2PIBS-Cu in order of precedence. Every substance under evaluation decreased the viability of cancer cells, also the type of metal ions present as well as geometrical configurations surrounding the central metal ions had a significant impact on this outcome **[32, 33].** The H_2PIBS-Cu complex beat the applied standard and showed strong and very encouraging anticancer activities against A-549 cell lines, with an IC50 value of 12.26 g/ml. Additionally, with an IC50 value of 13.43 g/mL, H_2PIBS-Cu showed the most promising result at Panc-1 cells. The results showed that the effectiveness of these compounds as potential anti-cancer agents for cancer cells is under investigation. (In 2023 Ani-Simona. S, et al) **[34]** used the (MTT assay) (a colorimetric assay for assessing cell metabolic activity) to assess the anti-proliferative impact from six azo-dyes also (TMZ) (Temozolomide resistance) in a human GB cell line at low passage. They discovered that all substances demonstrated antiproliferative effects on GB cells and they found that Azolo-dyes produced a more cytotoxic effect than TMZ at equimolar concentrations. Methyl Orange had the lowest IC50 for 3 days of treatment (26.4684 M), while Sudan I and Methyl Orange both had the highest potency for 7 days of treatment (13.8808 M and 12.4829 M, respectively). Under both experimental conditions, TMZ had the highest IC50. Conclusions: This work is innovative because it offers important insights into how azo-dye cytotoxicity affects high-grade brain cancers. This work may highlight azo-dye chemicals, which may represent a neglected source of therapeutic agents for the treatment of cancer.

How Azo-dye compound affects cell viability:

In this study, they looked at how different azo-dye compounds affected the ability of GB1B cells to grow in vitro. The concentration-effect relationship and associated IC50 values were examined using six azo-dyes: Sudan I, Methyl Orange, Alizarin Yellow, Butter Yellow, Lithol Rubine, and Methyl Red. Condensations of azo dyes ranged from 0.5 M to 128 M. At 3 and 7 days after the treatment, the MTT assay was used to measure the proliferation rates. Alizarin Yellow's Effect on Cell viability Our findings demonstrated that Alizarin Yellow caused GB1B cells to become cytotoxic at a dose- also time-dependent method. One of the examples is shown in **Figures 19 (A**

and **B**) this study showed none of the three concentrations out of nine used in this study significantly reduced cell viability at either 3 or 7 days.

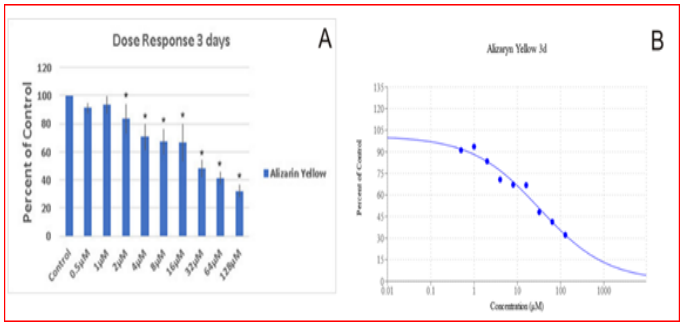

Fig – 19: Alizarin Yellow's effect on GB1B proliferation and calibration curves for IC50 is shown in Figures A and B, respectively, after three days of treatment. In a standard medium, 5 104 cells/well of cells were seeded. MTT assay has been utilized to assess the cytotoxic effects of Alizarin Yellow three days after treatment with increasing drug concentrations. Results are given as percentages compared to the control. The data shows the average and standard deviation across three different experiments. The error bars represent the linear model fit into data, that is the mean SD with each drug condensation. * Denotes a significant deviation from the control (p 0.05).

This study concludes that not much is known about the cytotoxic effects of azo-dye compounds on cancerous cells, and even less is known about their impact on brain tumors. The potential of certain azo dye compounds, like chemotherapeutic medications, for treating GB was only partially shown by in silico research. Currently, there aren't many experimental and theoretical articles about cytotoxic impact from azo-dyes at different types from cancer published at literature. The current study showed which azo-dye compounds had an anti-proliferative effect on GB cells in vitro and which compounds needed to be employed at lower dosages to have the same effects as TMZ, which was utilized as a reference medication when treating GB. That captures the novelty of the research. Due to their novelty, it is currently unclear if the studied azo-dyes could have the same impact in vivo as anticancer medicines. This work may highlight azo-dye compounds, which may be a neglected source of chemicals with anti-cancer properties. It would be fascinating to explore how they would effect other glioma subtypes and other malignancies both in vitro and in vivo, given their in vitro cytotoxicity on the GB cell line.

Conclusions:

According to the results of the recent synthesis and applications of various Azo dyes and their complexes, we can mention the following points. The UV-Vis studies showed that the new acid dye ligand complex of Cr (III), was octahedral geometry, with a good DNA binding mode and spontaneity compared to ligands. By diagnosing the new azo compound derived from 4-amino antipyrine, and 4-aminoacetophenone using analytical and spectroscopic methods, the complex revealed octahedral geometry and possesses appreciable microbial activities. Study and characterization of novel azo-linked benzoxazole, benzothiazole, and benzimidazole and docking studies that suggest these substances might develop into antibacterial agents in the future. Compared to Ciprofloxacin, comparative docking tests on common bacterial targets (PDB ids-2XCS and 1D7U) provide good docking outcomes. 8a was found to have a HOMO-LUMO gap. The low-cost chemical technique was used to manufacture the Zn(II) complex bound to the ligand, 5-amino-2,4-dichlorophenol-3,5-ditertbuthylsalisylaldimine. When the ligand is employed as a

sensitizer in a dye-sensitized solar cell device, it will have a power conversion efficiency. Therefore, it may be concluded that a cheaply manufactured Zn (II) metal Schiff-base complex could be used as a sensitizer in dye-sensitized solar cell systems. The present fluorescent probe shows high selectivity towards Al3+ and sufficiently low detection limits of 0.69 nM (WHO recommended values 7.41 mM) under healthy settings. Fortunately, the complex $[AlL_2]NO_3$ is 104 times more sensitive to F (LOD, 6.3 10 10 M) than the 3.9 10 6 M WHO recommended toxicity level. The HL exhibits an INHIBIT logic gate with Al3+ and F as chemical inputs by measuring the emission mode at 612 nm. Groundwater, a derivative of quinoline, azo, and naphthol (HL), has proven to be an effective fluorogenic probe that is incredibly specific in identifying Al^{3+} ions over other metal ions. Additionally, the catalyst's recycling process verified that the produced nanocatalyst is stable and that it can be retrieved and used at least seven times to reduce organic dyes by 100%. An analysis of the biological properties of thiazolyl azo ligand complexes containing metal ions revealed that the compounds exhibited antibacterial activity against the organism under study. For prepared compounds, an octahedral structure is recommended based on the outcome data. Cu (II), Zn (II), Co (II), and Ni (II) complexes containing azo ligands produced from metoclopramide hydrochloride are used in industry and biology. If research on antibacterial efficaciousness has been uploaded against the organism under test Depending on the desired result, dye and the compounds they formed were utilized in cotton fabric; a tetrahedral structure was suggested with the prepared compounds. The yields of the Thiophene-derived dyes produced in this work using Cu, Co, and Zn metal complexes were good, ranging from 63 to 99%. The polyester fabric has shown outstanding (5) fastness to perspiration and sublimation when dyes and their complexes were applied to it, whereas the nylon 6.6 fabric demonstrated very good (4) to excellent (5) fastness. The crystalline structure of polyester keeps color from escaping the fabric once it has entered it, which may be the cause of this variation in fastness. Nylon 6.6 and polyester were also found to have good to outstanding lightness and wash fastness. The intermediate amino thiophene is the source of these colors and compounds.Azo dye benzoic acid ligand derived from 2,4-dimethylphenol and 4-aminobenzoic acid, the ligand and compound addition has been used as dispersion dyes on cotton textiles to test the generated compounds' antibacterial efficacy against a variety of bacteria and fungus. They are expected to have four coordinated metal complexes and to be tetrahedral. Incorporation of Nickel with azo dye the produced NiL_2Cl_2 and $C_{23}H_{18}N_4O$ azo dye were examined in terms of their (morphological, structural, and optical characteristics) respectively, using photovoltaic parameters found from the I-V curve. As a result, $C_{23}H_{18}N_4O$ and NiL_2Cl_2 azo dyes can be employed as appropriate sensitizers when applying DSSCs. X-ray and spectroscopic investigations of two new azo-colorants made from phloroglucinol and antipyrine, and ten metal complexes containing [Cu (II), Co (II), Cd (II), Ni (II), and Zn (II)]. demonstrate that H_3L_1 exists in the azo tautomeric form and that it changes into H_3L_2, also referred to as tri-oxo di-hydroxylamine hydrazone, when nitrozated. The dissociation constants of both ligands at three different temperatures [298 K, 308 K, and 318 K] were calculated, and the thermodynamic functions of the dissociation process were determined. The newly synthesized azo generated from 2-hydroxy quinoline interacts with the following metal ions (Cr (III), Fe (III), Co (II), and Cu (II) to produce stable complexes with distinct geometries [tetrahedral for both Co (II) and Cu (II)], [octahedral for both Cr (III) and Fe (III)]. The results of the elemental microanalysis and the experimental earnings were extremely similar to the computed incomes. LC. The complexation is visible in the -Mss data through the -NO moiety. In addition to the results from other techniques,

the coordination of water residues with metal ions and chlorine atoms inside the coordination sphere was demonstrated by the pyrolysis (TGA & DSC) investigations. (FT-IR) of the compounds; as well as thermal analysis degradation stages. The lower the IC50 value, the higher the antioxidant activity.By this idea, our compounds, aside from Azo-species-HL, are arranged as follows: (G_A) $[Fe(L)(H_2O)_2Cl_2]$> [Cu(L) (H_2O) Cl]> [Cr(L) (H_2O) Cl]). Isolated azo dye complexes Cu (II), Ni (II), Co (II), Fe (III), and Zn (II) were created by reacting sulfafurazole diazonium chloride with resorcinol. (Analytical and spectroscopic) tools were utilized to investigate the structure of the isolated chelates. This resulted in the formation of the metal chelates in the following molecular formulas: $[Cu(H_2PIBS)_2(H_2O)_2]\cdot 1.5H_2O$, $[Ni(H_2PIBS)Cl(H_2O)_3]$, $[Co(H_2PIBS)Cl(H_2O)_3]$, $[Fe(H_2PIBS)Cl_2(H_2O)_2]$, and $[Zn(H_2PIBS)_2(H_2O)_2]$, where H_2PIBS abbreviates the mono-deprotonated ligand and thus indicating the formation of [1L: 1M] stoichiometry for Fe(III), Ni(II), and Co(II) chelates, and where Zn(II) and Cu(II) complexes formed in the ratio [2L: 1M]. The acquired data demonstrated that the most active ligands against the other strains tested were H_3PIBS and its complexes H_2PIBS-Cu and H_2PIBS-Zn. The molecular docking simulation of the compounds of interest with the Staphylococcus aureus adhesion protein receptor (PDB ID: 4m01) and these results agree well. Using two tumor cell lines, Panc-1 (pancreatic carcinoma) and A-549 (human lung carcinoma cancer cell line), the anticancer activity of the investigated compounds was evaluated.The results indicated that the metal complexes had greater antitumor activity than the parent ligand. The Cu (II) chelate has demonstrated encouraging activity against A-549 and Panc-1 cell lines in docking tests with caspase-3 (PDB ID: 2XYG), with IC50 values of 12.26 and 13.43 µg/ml, respectively. Viscosity and UV.Vis spectra studies have been used to investigate the mode of interaction of the compounds with DNA. The findings demonstrate that the Kb values and the rise in viscosity of the DNA solution following adding different doses of the chemicals under research reflect the intercalation mechanism of binding with SS-DNA.

References:

[1] Fateh. E, Nabil. B, Rajab. El-Kailany, and Nada. E, Aziza. A, Chemistry, and Applications of Azo Dyes: A Comprehensive Review, *Journal of Chemical Reviews* 2022, 4, 4: 313 – 330. http://doi.org/10.22034/JCR.2022.349827.1177 .

[2] Nagham. M. A, Aljamali. N .M, Nagham. M. A., Review in Azo Compounds and its Biological Activity, *Biochemistry & Analytical Biochemist* 2015,4, 2: 1-4. http://doi.org/10.4172/2161-1009.1000169 .

[3] Gung. B.W and Taylor. R, Parallel combinatorial synthesis of azo dyes: A combinatorial experiment suitable for undergraduate laboratories. *Journal of Chemical Education* 2004, 81: 1630 – 1632. http://doi.org/10.1021/ED081P1630 .

[4] Amer J. Jarad, Marwa Ali Dahi, Taghreed H. Al-Noor, Marei M. El-ajaily, Salam R. AL-Ayash, Aly Abdou, Synthesis, spectral studies, DFT, biological evaluation, molecular docking and dyeing performance of 1-(4-((2-amino-5-methoxy) diazenyl) phenyl) ethanone complexes with some metallic ions, *Journal of Molecular Structure* 2023, *1287*, 1-16. http://doi.org/10.1016/j.molstruc.2023.135703

[5] 5 – Ho M. S., Barrett. C, Paterson. J, Esteghamatian .M, Natansohn . A, and Rochon. P, Synthesis and Optical Properties of Poly{(4-nitrophenyl)-[3-[N-[2-(methacryloyloxy)ethyl]-carbazolyl]]diazene} , 1996, 29, 13: 4613–4618. https://doi.org/10.1021/ma951432a .

[6] 6 - Yin, S.; Xu, H.; Shi, W.; Gao, Y.; Song, Y.; Lam, J. W. Y.; Tang, B. Z, Synthesis and Optical Properties of Polyacetylenes Containing Nonlinear Optical Chromophores, *Polymer* 2005, 46, 7670–7677. https://doi.org/10.1016/j.polymer.2005.05.118 .

[7] 7 –Peter. B, Chromic phenomena. The Technological Applications of Colour Chemistry, The Royal Society of Chemistry, Cambridge.UK, 2001 P: 80-111.

[8] 8- Nasir A, Syed A. Tirmizi, Ghulam S, Aamer S, Ghulam H, Pervaiz A. Channer, Rashid S, and Uhammad A, Chromium (III) complexes of azo dye ligands: Synthesis, characterization, DNA binding and application studies, *Inorganic and Nano-Metal Chemistry*, 2017, 47 (1):1-33. http://dx.doi.org/10.1080/24701556.2017.1357632 .

[9] 9- Jinan M, Mahmood AL-Zinkee and Amer J. Jarad, Synthesis, Characterization and Microbial Evaluation of Heterocyclic Azo Dye Ligand Complexes of Some Transition Metal (II) Ions, *Asian Journal of Chemistry* 2019, 31(3): 727-732. https://doi.org/10.14233/ajchem.2019.21800 .

[10] 10- Martina Di Matteo, Barbara. P, Stefano. P, and Simona. C, Azobenzene as Antimicrobial Molecules, *Molecules* 2022, 27(17): 1-30. https://doi.org/10.3390/molecules27175643.

[11] 11- Virendra R. Mishraa, Chaitanya W. Ghanavatkara, Suraj N. Malib, Shahnawaz I. Qureshia,b, Hemchandra K . , and Chaudharib, Sekara, Design, synthesis, antimicrobial activity and computational studies of novel azo linked substituted benzimidazole benzoxazole and benzothiazole derivatives, *Computational Biology and Chemistry* 2019, 78:330–337.

[12] https://doi.org/10.1016/j.compbiolchem.2019.01.003 .

[13] 12- Dilek K,· Ömer Ş , and Sabit H , Use of low‐cost Zn(II) complex efficiently in a dye‐sensitized solar cell device. *Journal of Materials Science: Materials in Electronics* 2019, 30:11464–11467. https://doi.org/10.1007/s10854-019-01497-5 .

[14] 13 – Chandana. S, Sunanda. D, Chiranjit. P, Debashis. M, and Chittaranjan. S, use of the fluorogenic Al^{3+}-quinolinyl-azonaphtholato complex for the determination of F^- in aqueous medium by visible light excitation and application in groundwater fluoride analysis, *Analytical Methods* 2019, 11: 4440–4449. http://doi.org/10.1039/c9ay01418g.

[15] 14- Farhana. A, Saima. G, Mohammad I. K, and Murad A. K, Efficient synthesis of palladium nanoparticles using guar gum as a stabilizer and their applications as a catalyst in reduction reactions and degradation of azo dyes, *journal Green Processing and Synthesis* 2020, 9, 1: 63 – 76. https://doi.org/10.1515/gps-2020-0008 .

[16] 15 – Marwa A. D, and Amer J. J., Synthesis, characterization and biological evaluation of thiazolyl azo ligand complexes with some metal ions. *Journal of Physics: Conference Series* 2020,1664. http://doi.org/10.1088/1742-6596/1664/1/012090.

[17] 16- Shatha M. H Obaida, Afnan E.Abd-Almonuimb, Amer J.J, Synthesis, Characterization, Industrial And Biological Application of Co(II), Ni(II), Cu(II) And Zn(II) Complexes With Azo Ligand Derived From Metoclopramide Hydrochloride And 3,5-Dimethylphenol, *Egyptian Journal of Chemistry* 2020, 63, 12: 4719-4729. http://doi.org/10.21608/EJCHEM.2020.21400.2283 .

[18] 17 - Isaac O. A, Kasali A. B, Peter O.N, and Abdulraheem G, Complexation of Disperse Dyes Derived from Thiophene with Cu, Co, Zn Metal and Their Application Properties on Polyester and Nylon 6.6 Fabrics, *American Journal of Science, Engineering and Technology* 2021, 6, 3: 50-63. http://doi.org/10.11648/j.ajset.20210603.11.

[19] 18 - Abaas O. H, Rana A. A., Jasim S. S, and Amer J. J, Synthesis and Characterization of Metal (II) Complexes with Azo Dye Ligand and Their Industrial and Biological Applications, *Egyptian Journal of Chemistry* 2021, 64, 11:6717 – 6724. http://doi.org/10.21608/EJCHEM.2021.68770.3530 .

[20] 19 - Eman H. S, Fatima A. A. S, and Hutham M. Y. Al-Labban, Incorporation of Nickel with Azo Dye and its Applications in Dye-Sensitized Solar Cells, *International Journal of Drug Delivery Technology* 2022,12,2:603-609.

[21] http://doi.org/10.25258/ijddt.12.2.24 .

[22] 20 - Anh V. N, Anh T. N. V, bi Liya V. Bazan, C Ravil T. G, C Andrey N. U, d Ekaterina B. M, e Van T. L. gh, and Olga V. K, Synthesis, characterization, and sorption activity of novel azo-colorants derived from phloroglucinol and antipyrine and their metal complexes, *Royal Society of Chemistry* 2022, 12: 888-898. http://doi.org/10.1039/d1ra07254d .

[23] 21 – Adhraa G. A, and Abbas A. S Al –Hamdani, Cr (III), Fe (III), Co (II) and Cu (II)Metal ions Complexes with Azo Compound Derived from 2-hydroxy Quinoline Synthesis, Characterization, Thermal Study and Antioxidant Activity, *Ibn Al-Haitham*

Journal for Pure and Applied Sciences 2023, 36,3: 214-230. http://doi.org/10.30526/36.3.3068 .

[24] 22 - Hoda A. El-Ghamry, Rajaa O. Al-Ziyadi, Fatmah M. A, Khadija M. T, and Abdalla M. K, Metal Chelates of Sulfafurazole Azo Dye Derivative: Synthesis, Structure Affirmation, Antimicrobial, Antitumor, DNA Binding, and Molecular Docking Simulation, Bioinorganic Chemistry and Applications 2023, 2023. https://doi.org/10.1155/2023/2239976.

[25] 23 - Hoda A. El-ghamry, Khadiga. M. T, Dalal. O. Al-Rashidi, Elaf. S. A, and Reem. A. A, Design, spectral, thermal decomposition, antimicrobial, docking simulation and DNA binding tendency of sulfisoxazole azo dye derivative and its metal chelates with Mn^{2+}, Fe^{3+}, Co^{2+}, Ni^{2+}, Cu^{2+}, Zn^{2+} and Cd^{2+}, *Applied Organometallic Chemistry* 2022, 36, 9: e6813. https://doi.org/10.1002/aoc.6813.

[26] 24 – Hossein. J, Jelas. H, Mohd .H, Mohd.H. S.I, and Roshanak. R. M, Well diffusion method for evaluation of antibacterial activity, *Digest Journal of Nanomaterials and Biostructures* 2013, 8, 3: 1263–1270.

[27] 25 - Abdall. M. K, Ayman. A. G, and Hoda. A. El-Ghamry, Nano-synthesis approach, elaborated spectral, biological activity and in silico assessment of novel nano-metal complexes based on sulfamerazine azo dye, *Journal of Molecular Liquids*, 2022, 352. https://doi.org/10.1016/j.molliq.2022.118737 .

[28] 26 – Mohamed. G, Abdalla. M. K, Mohammed. A. M, and Mohsen. E, Nano-synthesis, characterization, modeling and molecular docking analysis of Mn (II), Co (II), Cr (III) and Cu (II) complexes with azo pyrazolone ligand as new favorable antimicrobial and antitumor agents, *Applied Organometallic Chemistry*, 2018, 32, 12: 4606. https://doi.org/10.1002/aoc.4606.

[29] 27 – Singh B. K., Jetley U. K, Sharma R. K, and Garg B. S, Synthesis, characterization and biological activity of complexes of 2-hydroxy-3,5-dimethylacetophenoneoxime (HDMAOX) with copper (II), cobalt (II), nickel (II), and palladium(II), *Spectrochimica Acta Part A: Molecular and Biomolecular Spectroscopy* 2007, 68, 1: 63–73. https://doi.org/10.1016/j.saa.2006.11.001 .

[30] 28 - Tania. G, and Muhammad. H, Metal-based complexes in cancer treatment, Biomedicines 2022,10: 2573–2578.https://doi.org/10.3390/biomedicines10102573

[31] 29- AL-Musawi, M, Khoshkalampour, A., AL-Naymi. H.A, Shafeeq,Z.F., Doust, S.Ghorbani, M. (2023). Optimization and characterization of carrageenan/gelatin-based nanogel containing ginger essential oil enriched electrospun ethyl cellulose/ casein nanofibers. Int, journal Biol macromol, 125969. Doi: 10.10.16/j.ijbiomac.2023.125969.

[32] 30- Hoda. A. El-Ghamry, Bushra. K. A, Khadiga.T, and Abdalla. M. K, A series of nanosized Cu (II) complexes based on sulfonamide azo dye ligands: an insight into complexes molecular structures, antimicrobial, antitumor and catalytic performance for oxidative dimerization of 2-aminophenol, *Applied Organometallic Chemistry*, 2022, 37, 2: 6978. http://doi.org/10.1002/aoc/6978.

[33] 31 - Abdalla M. K, Hoda El-Ghamry, Mohammed A. K, Fawaz A. S, N. El-Guesmi, Novel series of nanosized mono- and homo bi-nuclear metal complexes of sulfathiazole azo dye ligand: Synthesis, characterization, DNA-binding affinity, and anticancer activity, *Inorganic Chemistry Communications* 2019, 108, https://doi.org/10.1016/j.inoche.2019.107496.

[34] 32 - Fawaz. A. S, Hoda. A. El-Ghamry, Mohammed. A. Kassem, and Abdalla. M. K, Nano-synthesis, biological efficiency and DNA binding affinity of new homo-binuclear metal complexes with sulfa azo dye-based ligand for further pharmaceutical applications, *Journal of Inorganic and Organometallic Polymers and Materials*,2019, 29, 4: 1337–1348. https://doi.org/10.1007/s10904-019-01098-z .

[35] 33- Al-Naymi, N.A.Sh., Al- naymi, H.A.S. and Nashaat,M.R .,(2022) Toxicity Stress of the Durah Power Plant Ash and its Effect on the Alga Chlorococcum humicola (Naeg) Rabenhorst 1868. Arab Journal of Plant Protection, 40(2): 188-192.

[36] 34 - Ani-Simona. S, Carina. B, Oana. A, Ligia. G.T, Oana. S. P, and Anica. D, The effect of Azo-dyes on glioblastoma cells in vitro, *Saudi Journal of Biological Sciences* 2023, 30,3: 103599. http://doi.org/10.1016/j.sbs.2023.103599 .